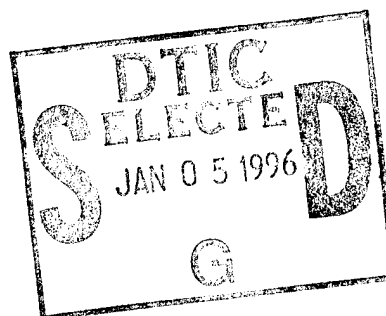Defense Nuclear Agency
Alexandria, VA 22310-3398

DNA-TR-94-174

Evaluation of Temperature Compensated Bubble Dosimeters for Treaty Verification Applications

ENS Bradford W. Baker, USN
Dr. Mark J. Harper
Dr. Martin E. Nelson
United States Naval Academy
Department of Naval Architecture
Ocean and Marine Engineering
590 Holloway Road
Annapolis, MD 21402

DTIC
SELECTE
JAN 0 5 1996
G

19951229 002

December 1995

Technical Report

DTIC QUALITY INSPECTED 3

REPORT DOCUMENTATION PAGE

Public reporting burden for this collection of information is estimated to average 1 hour per response, including the time for reviewing instructions, searching existing data sources, gathering and maintaining the data needed, and completing and reviewing the collection of information. Send comments regarding this burden estimate or any other aspect of this collection of information, including suggestions for reducing this burden, to Washington Headquarters Services, Directorate for Information Operations and Reports, 1215 Jefferson Davis Highway, Suite 1204, Arlington, VA 22202-4302, and to the Office of Management and Budget, Paperwork Reduction Project (0704-0188), Washington, DC 20503.

1. AGENCY USE ONLY (Leave blank)	2. REPORT DATE 951201	3. REPORT TYPE AND DATES COVERED Technical 930601 – 940930

4. TITLE AND SUBTITLE

Evaluation of Temperature Compensated Bubble Dosimeters for Treaty Verification Applications

5. FUNDING NUMBERS

C – DNA-MIPR-92-714

6. AUTHOR(S)

Bradford W. Baker, Mark J. Harper and Martin E. Nelson

7. PERFORMING ORGANIZATION NAME(S) AND ADDRESS(ES)

United States Naval Academy
Department of Naval Architecture
Ocean and Marine Engineering
590 Holloway Road
Annapolis, MD 21402

8. PERFORMING ORGANIZATION REPORT NUMBER

9. SPONSORING/MONITORING AGENCY NAME(S) AND ADDRESS(ES)

Defense Nuclear Agency
6801 Telegraph Road
Alexandria, VA 22310-3398

VTSA/Simelton

10. SPONSORING/MONITORING AGENCY REPORT NUMBER

DNA-TR-94-174

11. SUPPLEMENTARY NOTES

12a. DISTRIBUTION/AVAILABILITY STATEMENT

Approved for public release, distribution is unlimited.

12b. DISTRIBUTION CODE

13. ABSTRACT (Maximum 200 words)

Due to drawdown of nuclear weapons through treaties among countries and the possible proliferation of nuclear weapons to the Third World, the Defense Nuclear Agency is investigating different methods that can be used to distinguish nuclear from non-nuclear munitions. Due to its small size, lack of electronics, and non-obtrusive data collection capability, the bubble dosimeter is a candidate for this process.

The objective of this research is to investigate the response of alternate droplet material bubble dosimeters as it pertains to arms control verification procedures. This was accomplished by theoretically and experimentally studying (1) the bubble dosimeter's response to warhead neutron intensity and energy, (2) the bubble dosimeter's sensitivity to gamma radiation, (3) the bubble dosimeter's response as a function of temperature, and (4) the bubble dosimeter's response as a function of neutron energy.

14. SUBJECT TERMS

Bubble Dosimeter   Data Analysis   Gamma Radiation
X-Rays   Plutonium   Uranium

15. NUMBER OF PAGES 112

16. PRICE CODE

17. SECURITY CLASSIFICATION OF REPORT	18. SECURITY CLASSIFICATION OF THIS PAGE	19. SECURITY CLASSIFICATION OF ABSTRACT	20. LIMITATION OF ABSTRACT
UNCLASSIFIED	UNCLASSIFIED	UNCLASSIFIED	SAR

NSN 7540-01-280-5500

Standard Form 298 (Rev. 2-89)
Prescribed by ANSI Std 239-18
298-102

SECURITY CLASSIFICATION OF THIS PAGE

CLASSIFIED BY:
N/A since Unclassified

| DECLASSIFY ON: | N/A since Unclassified |

13. ABSTRACT (Continued)

Conclusions are drawn regarding the potential use of bubble dosimeters for treaty verification applications. Through research on simulated warhead sources, practical procedures are outlined for using the bubble dosimeter to distinguish nuclear from non-nuclear munitions.

Acknowledgements

The assistance of several people needs to be mentioned here. First, a special thanks is extended to LTCOL Benard Simelton, of the Defense Nuclear Agency, for the sponsorship of this research, as well as Ed Hamilton and John McNeilly of the Center for Verification Research, for their support and supervision.

A special thanks is extended to Bill Johnson and Wayne Fehlau of Los Alamos National Laboratory, CAPT Galley of the Armed Forces Radiobiological Research Institute, Jack Price and Noel Guardala of Naval Surface Warfare Center for their help in the operations with their respective facilities.

A special thanks is extended to Mike Gibbons whose mechanical expertise made all operations at the United States Naval Academy run smoothly.

Lastly, thank you to Clarissa for your unending support and patience.

Accesion For		
NTIS CRA&I		☒
DTIC TAB		☐
Unannounced		☐
Justification		
By		
Distribution /		
Availability Codes		
Dist	Avail and / or Special	
A-1		

1

Table of Contents

Chapter IV - Temperature Response Studies

Chapter V - Neutron Energy Studies

Chapter VI - Conclusions and Recommendations

List of Tables

List of Figures

5

Nomenclature

Abbreviations:

AFRRI	Armed Forces Radiobiological Research Institute
AmLi	Americium Lithium neutron source
ASM	Apfel Surveymeter
BTI	Bubble Technology Industries
Cf^{252}	Californium-252 neutron source
Co^{60}	Cobalt-60 gamma source
DNA	Defense Nuclear Agency
HFC	HFC-134A droplet material bubble dosimeter
HFP	Hexafluoropropylene droplet material bubble dosimeter
LANL	Los Alamos National Laboratory
NELA	Nuclear-Explosive-Like Assembly
NSWC	Naval Surface Warfare Center
R-12	R-12 droplet material bubble dosimeter
SARA	Service Academy Research Associates
SDD	Superheated Drop Detector
USNA	United States Naval Academy

Variables:

CF_{sens}	Correction factor for sensitivity degradation of Apfel dosimeters
CF_{time}	Correction factor for time
$D_{initial}$	Initial number of droplets in Apfel dosimeter
D_{final}	Final number of droplets in Apfel dosimeter
E_a	Energy deposited by recoil ion
E_c	Critical energy required to form a bubble
E_n	Neutron energy
E_p	Proton energy
E_{th}	Threshold energy
P_{cor}	Time and sensitivity corrected number of pops
P_{raw}	Raw number of pops from ASM
σ	Standard deviation, cross section
T_{ASM}	Time measured from ASM
TCF	Temperature Correction Factor
θ	Emission angle in laboratory system

Chapter I

Background and Objectives

A potential application of bubble dosimeters for arms control verification regimes is described. Two bubble dosimeter types are described. The objectives of the research reported herein are outlined.

1.1 Arms Control Verification Methods

Due to the recent collapse of the Soviet Union and the drawdown of nuclear weapons through the Strategic Arms Reduction Treaty (START), an accurate method of distinguishing nuclear munitions from non-nuclear munitions is being sought to prevent the proliferation of nuclear weapons throughout the world. Current and potential methods of arms control verification include radiographic, gravimetric, and acoustic processes.[1] These methods are often difficult to use in actual field environments due to the cumbersome electrical or mechanical equipment required to perform them. Another disadvantage of these procedures is that they may reveal information about the weapon other than simply the presence or absence of nuclear material, which may result in a country, including the United States, disallowing their use for security reasons. To overcome these problems, it is desired to have a non-intrusive device that can be used in a field environment that can differentiate between nuclear and non-nuclear munitions.

All fissile nuclear materials emit one or more types of radiation, including alpha and beta particles, neutrons, and photons (x-rays and gamma rays). The presence of plutonium and uranium in nuclear munitions produces neutrons and gamma rays. These radioactive emissions are capable of penetrating encapsulating materials with varying degrees of attenuation. For example, alpha and beta particles as well as low energy photons are unable to penetrate virtually any shielding configuration, while the neutrons or high energy gamma rays, characteristic of plutonium or uranium, are capable of penetrating the casings of nuclear munitions. For these reasons the detection of alpha or beta particles or low energy photons is useful for the detection of bare sources, while the detection of neutrons or gamma rays is useful for the detection of fully assembled nuclear munitions.

Treaty verification based on emitted nuclear radiation was established under the Intermediate-Range Nuclear Forces (INF) Treaty and was accepted by the former Soviet Union.[2] Under the INF Treaty, allowed SS-25 missiles were distinguished from banned SS-20 missiles using neutron detection methods. Additionally, research at Los Alamos National Laboratory (LANL) has been conducted to distinguish between nuclear and non-nuclear munitions based on emitted radiation from nuclear-explosive-like assemblies (NELAs).[3,4] The NELA is a laboratory device that resembles a nuclear assembly but does not contain any high explosives. Radiation readings taken from NELAs are realistic and

representative of actual nuclear assemblies. The NELAs at LANL were used in this research as representative models of nuclear assemblies and are referred to as special sources.

The instrument currently used at LANL for verification of the NELAs is the NNV-470. The NNV-470 is a small hand portable battery operated radiac used to measure radiation readings around nuclear material. The NNV-470 uses a moderated, 2.5 cm diameter, enriched lithium iodide [$Li^6I(Eu)$] scintillator to convert neutrons and gamma rays into light, which is then converted to current.[3] The NNV-470 is sensitive to thermal neutrons and gamma rays and uses a voltage level discriminator to distinguish the large pulses produced by neutrons from the small pulses produced by gamma rays. The NNV-470 counts for 20 seconds and then displays the total number of counts on a LCD display.

In addition to the NNV-470, which is used to verify non-nuclear munitions by the absence of neutrons, there are devices such as the TSA Systems MCA-465 which verify non-nuclear munitions based on the absence of emitted gamma rays.[3] The MCA-465 is a hand portable, battery operated multi-channel analyzer that uses either an internal or external NaI(Tl) detector for identifying gamma ray emitting materials. The MCA-465 is more useful in the detection of materials containing only highly enriched uranium due to the U^{232} daughter gamma rays produced, while the NNV-470 is more suited for materials that contain plutonium due to their emission of neutrons.

Another candidate for arms control verification is the bubble dosimeter which detects fast neutrons. Because of its small size, simple construction, and non-intrusive data collection capability, the bubble dosimeter is also a candidate for field use. Past research has been conducted at the United States Naval Academy (USNA) to investigate the feasibility of using bubble dosimeters for arms control verification.[1]

1.2 Bubble Dosimeters

The bubble dosimeter is a radiation measuring device that operates on the same theory as bubble chambers with the fundamental difference being that bubble dosimeters consist of many superheated liquid droplets suspended in a gel material. Each individual superheated liquid droplet in the bubble dosimeter acts as an individual bubble chamber, wherein the gel material serves as a restraint for the liquid droplets. This allows the liquid to remain in the superheated state for an extended period of time. Choosing a shock-absorbing gel material causes the vaporization of the individual droplets to be a singular event in that the nucleation of adjacent droplets is prevented. This allows the incident radiation to be quantified by counting the bubbles formed. Varying the density of droplets within the dosimeter or the droplet material serves as a method of varying the sensitivity of the bubble dosimeter.

There are currently two different bubble dosimeter types commerically available:

the Apfel superheated Drop Detector (SDD)[5], a product of Apfel Eterprises, and the

Bubble Technology Industries (BTI) bubble dosimeter, designed by Ing.[6] Both dosimeters

operate on the principles mentioned previously with their difference being how the

vaporization events are counted.   The Apfel SDD dosimeter is a small glass vital (4 ml)

which contains approximately 24,000 superheated liquid droplets suspended in a semi-solid

mixture of water, glycerine, and gel.[7] Neutron interactions within the SDD result in the

vaporization of the droplet material and the formation of vapor bubbles. Each bubble

formation is accompanied by an acoustic pressure pulse called a "pop".[7] Because the

droplets are not rigidly confined in the gel material, the bubbles slowly rise out of the gel

once formed. Because the bubbles dissipate within the SDD after formation, the

sensitivity of the dosimeter, which is proportional to the number of droplets remaining,

will decrease over time, which results in a limited useful lifetime of the SDD. Apfel's

original SDD is the SDD-100 which uses R-12 as the droplet material.

After further research by Apfel and Rich, Apfel has produced both the

SDD-100S and the SDD-10 which contain HFC-134A (HFC) and hexafluoropropylene

(HFP) respectively as droplet material. These dosimeters were studied in this research

and are referred to as R-12, HFC, and HFP respectively.

The Apfel SDD dosimeter is used in conjunction with the Apfel Surveymeter

(ASM) to measure neutron dose. The ASM is a portable device that electronically records

each pop by means of a piezoelectric transducer.[8] The signal from the transducer is sent through discrimination and anti-coincidence circuitry before entering the counting circuitry. The ASM also translates the recorded pops into neutron dose equivalent which is digitally displayed on the ASM. There are currently two ASM models (01 and 02) commercially available. The 01 and 02 models operate identically with the only difference being the readout of the ASM. The 01 model allows only for a readout of accumulated dose while the 02 model allows for a direct readout of pops as well as accumulated dose. Detailed information on the design and theory of the Apfel SDD and ASM is available in open literature.[7,9]

The BTI bubble dosimeter is a small test tube shaped device approximately 14 cm long. The bottom half of the BTI dosimeter (approximately 6 cm long) is transparent and houses the gel material which contains the superheated liquid droplets. Unlike the Apfel device, the gel material in the BTI dosimeter is a rigid polymer which does not allow the bubbles to move once formed. It contains enough superheated droplets so that once the bubbles are formed they can be seen with the naked eye and counted either visually or with an optical reader. Because the droplets never leave the dosimeter once they form the bubbles, the BTI dosimeter can be reused with no degradation in sensitivity by repressurizing the dosimeter which causes the bubbles to recondense. The top of the BTI dosimeter is fitted with a mechanical piston to create pressure on the gel material to

13

prevent formation of bubbles or to recondense bubbles that are already formed. The piston of the BTI is activated by unscrewing the top cap of the dosimeter, reversing its direction, and screwing it back on hand tight.

The neutron dose equivalent from the BTI dosimeter is calculated by counting the number of visible bubbles formed within the dosimeter, either visually or by using the bubble reader designed by BTI, and dividing by the sensitivity of the detector. The sensitivity of each individual BTI dosimeter is determined experimentally by BTI after manufacture and is written on each dosimeter in bubbles per mrem (bub/mrem).

One of the problems associated with the bubble dosimeter's use has been its response with changing temperature. The response of both the Apfel and BTI dosimeters have proven to be non-linear with increasing temperature.[1,10] This temperature dependence problem has been approached in several different ways. Buckner and Harper both discuss possible ways of maintaining a constant temperature around the dosimeter as a means to solve this problem.[10,11] The BTI dosimeter incorporates a temperature compensating fluid, while the ASM uses an additional equation in its algorithm to compensate for temperature. This allows both of the dosimeters to give a reading that has been corrected for temperature. However, neither of these approaches is entirely effective because the BTI compensating fluid has a limited range and the Apfel computer algorithm assumes a known neutron source energy. The root cause of the temperature dependence lies in the

superheated droplet material. Rich has approached the problem at its source by researching alternate droplet materials that might give a constant response within a useful temperature band.[1] From the conclusions in Rich's report, Apfel has produced the HFC and HFP dosimeters designed to give an improved temperature response.

Another important effect of the bubble dosimeters, if they are to be used for treaty verification applications, is their response to gamma radiation. This response is important because it is expected that nuclear material would give a mixed field of neutron and gamma radiation. If the bubble dosimeter were responsive to gamma radiation, it would be impossible to differentiate between the responses due to neutrons and gamma rays. This would make it impossible for the bubble dosimeter to verify that a material was fissile. Additionally, detailed information on the gamma spectrum emitted from a device could reveal critical design features.

There is no evidence in the Harper model to suggest that the bubble dosimeter would give any response to gamma radiation. In research by Sisk et al., the Apfel dosimeter did not give any response to x-rays.[12] Similarly in the research by Millet et al., no response was recorded on the BTI dosimeter from a Co^{60} gamma source.[13] However, neither of these studies involved re-use of the dosimeters.

1.3 Research Objectives

It is the objective of this research to study the suitability of the bubble dosimeter for arms control verification by determining: (1) the bubble dosimeter's response to warhead neutron intensity and energy, (2) the bubble dosimeter's sensitivity to gamma radiation, (3) the bubble dosimeter's response as a function of temperature, and (4) the bubble dosimeter's response as a function of neutron energy.

The initial research for this report was conducted during an internship with LANL through the Service Academy Research Associates (SARA) program during the summer of 1993, which involved irradiating the bubble dosimeters by placing them around special sources (the NELAs at LANL). The purpose of this research was to determine the bubble dosimeters' response to warhead neutron intensity and energy as well as any procedures that would be required for actual field use. Results of this research are contained in Chapter II.

To determine the gamma sensitivity of the bubble dosimeters, both the Apfel and BTI dosimeter were irradiated with a Co^{60} source at varying distances. This test was conducted at the Armed Forces Radiobiological Research Institute (AFRRI) in Bethesda, Maryland. To determine the dosimeters' gamma sensitivity as a function of re-use the tests were conducted with dosimeters with a varying irradiation history. This was accomplished by alternating the neutron and gamma exposure to both dosimeters as well

16

as the repressurization sequence of the BTI dosimeter. Results of the gamma sensitivity tests are contained in Chapter III.

Based on Rich's investigation, Apfel has conducted research using alternate droplet materials in the SDD. Apfel has performed solubility tests on HFC, propylene, and propane to determine if they are compatible with his gel material. Apfel has determined that, of these three candidate materials, only HFC is stable in his gel material. Additionally Apfel has proposed the use of HFP as a droplet material. The dosimeters with these two new droplet materials are designed to have a decreased temperature dependence. The dosimeters with the alternate droplet materials and new 02 model ASM were studied at USNA to determine their temperature response by irradiating the dosimeters at varying temperatures. Results of the temperature studies are contained in Chapter IV.

The final phase of this research is to determine the response of the new and old design Apfel dosimeters as a function of neutron energy. To determine this response, the Apfel dosimeters were irradiated with varying neutron energies with a tandem proton accelerator and a lithium target located at the Naval Surface Warfare Center (NSWC) in White Oak, Maryland. Results of the neutron energy tests are contained in Chapter V.

Chapter II

Bubble Dosimeter Response to Special Sources

The objective of the research at LANL is given. The individual tests conducted are described. Results and conclusions are given concerning the BTI bubble dosimeter's response to warhead neutron intensity and energy.

2.1 Introduction

The objective of this research is to determine the response of the BTI and Apfel bubble dosimeters to warhead neutron intensity and energy and to determine practical procedures for the bubble dosimeter to be used for arms control verification. This research was conducted at LANL through a summer internship. To complete this research, 100 BTI BD-100R dosimeters, 25 Apfel SDD-100 dosimeters, the Apfel surveymeter, and a portable computer were sent to LANL. An optical scanner was available through LANL Tech Area 55 for reading the BTI dosimeters. Upon arrival at LANL it was discovered that the Apfel surveymeter had been damaged in shipment and had to be returned to Apfel Enterprises to be repaired. Because of this, insufficient data was obtained with the Apfel dosimeter, and no conclusions on the Apfel dosimeters were possible while at LANL.

2.2 Test Plan

Table 2.1 - Summary of LANL Tests

Test Number	Irradiation Source	LANL Location
2.1	Background	ADL
2.2	Background	Kiva 2
2.3	Cf^{252}	ADL
2.4	Cf^{252}	ADL
2.5	AmLi	ADL
2.6	Special Source 1	Kiva 2
2.7	Special Source 1	Kiva 2
2.8	Special Source 2	Kiva 2
2.9	Special Source 2	Kiva 2

While at LANL, 9 experiments were conducted. Table 2.1 lists each test performed, its irradiation source, and location. The Cf^{252} irradiations (Tests 2.3 and 2.4) were planned to be tie points of research between LANL and USNA since these experiments could be repeated at USNA. The Cf^{252} source used at LANL produced $2.5*10^4$ neutrons per second but did not produce a significant number of bubbles in the dosimeters even after long periods of irradiation. Because of this, the Cf^{252} experiments provided little valuable information on the performance of the BTI dosimeters and will not be discussed in this report.

In each experiment the main objective was to calculate a count rate in bubbles per hour (bub/hr) produced by each source for each dosimeter. This was accomplished by

dividing the number of bubbles within the dosimeter by the irradiation time for each source to yield bubbles per hour. For ease of calculation and comparison this value was then normalized to a bubble dosimeter having a sensitivity of 50 bubbles per mrem by multiplying by the ratio of 50 to the sensitivity of the individual device written on the dosimeter. In these tests, most devices had sensitivities ranging between 30 to 50 bubbles per mrem. For all tests the background radiation reading for that test area was subtracted from the calculated count rate to yield a count rate in bubbles per hour above background.

2.3 BTI Bubble Reader[14]

One of the past problems associated with using the BTI dosimeters has been unfamiliarity with the bubble reader. Questions as to which commands or settings gave the most accurate counting methods have created difficulties in using the bubble reader. This problem was studied while at LANL, and all techniques regarding the bubble reader were documented at the time of each batch reading.

The bubble reader includes two cameras, one of which is focused on the upper half of the dosimeter while the other is focused on the lower half. The reader defines a bubble as a region of white surrounded by a region of black which in turn is surrounded by another region of white. The inner region of white represents the encapsulated area of the bubble, the region of black represents the bubble wall, and the outer region of white

20

represents the region outside of the bubble. Areas in a dosimeter having no bubbles are displayed white.

When the reader is given the command to count the entire sample, it displays the upper camera image, places a small white box at each point that it determines is a bubble, and then displays the total number of bubbles which is equal to the number of white boxes on the screen. This process is then repeated for the lower camera, and the two numbers are added together to give a final count for the entire dosimeter. By watching the screen as the reader places the white boxes, the operator can determine whether the reader is accurately counting the dosimeter yield or not. It is possible that the reader is not placing boxes where there are bubbles or that the reader is placing too many boxes on a number of bubbles.

Four of the instrument functions that the operator can control to affect the bubble count are maximum and minimum white blob area and maximum and minimum black blob area. These functions determine the maximum and minimum number of pixels that must be present for a given area to be considered white or black. An example of the importance of these values is the minimum white blob area. If the area encapsulated by a bubble is smaller than the minimum white blob area, then the bubble is displayed solid black and therefore will not be counted, i.e. it will not receive a white box. Similarly if a section of a bubble wall is smaller than the minimum black blob area, the bubble will not be

displayed as a full circle and therefore will also not be counted. Similarly the bubble will not be counted if its white or black area exceeds the corresponding maximum blob area. After discussion with George Neuman, the operator of the bubble reader at LANL Tech Area 55, the following defaults were set and not changed at any time:[15]

Minimum White Blob Area =   10

Maximum White Blob Area =   500

Minimum Black Blob Area =   20

Maximum Black Blob Area =   500

Values similar to these have been used in past bubble dosimeter studies at USNA.[1,16,17]

Another operator controlled reader function is the detection threshold setting. The detection threshold determines what degree of white the reader determines is white and what degree of black the reader determines is black. A lower detection threshold causes more shades to be determined white and a higher threshold causes more shades to be determined black. The detection threshold in each camera is independent of the other camera, and the value for each camera's detection threshold is used when the command "count sample" is given. This allows the operator to set a detection threshold in each camera that gives an accurate counting of that camera's image as observed by the placement of boxes around the bubbles. The operator sets a detection threshold in each camera before the reader counts the entire sample. Normal values used for detection

22

thresholds range from 55-75 as determined by this research, George Neuman's experience, and past research at USNA.[1,15,16,17]

There are a variety of factors that complicate the bubble reading process. One of these factors is lens and dosimeter condition. It was found during one experiment that the bubble reader continually displayed one camera image darker than the other. This problem was not alleviated even after cleaning both the dosimeter and the lens. Another complicating factor is the number of bubbles. The more bubbles there are in a sample, the more bubble shielding and bubble merging become problems. The size of the bubbles also directly affects the shielding and merging problems. It has been proven in past research that bubbles grow after being formed, thus time after irradiation becomes a factor in the bubble reading problem.[1]

Because of these problems with bubble counting, a specific method was adopted and adhered to when using the bubble reader. First, the defaults for blob areas were set as determined by George Neuman's defaults and were never changed. Next, for each dosimeter, both the upper and lower cameras were assigned independent detection threshold settings. This was accomplished by looking at each camera image, and changing the threshold as necessary until an accurate counting scheme was visually observed for that camera image by the placement of the boxes on the bubbles. Once both cameras had set detection threshold settings, the entire sample was counted to yield the number of bubbles

in the dosimeter. The dosimeter was then rotated 90 degrees and counted again without changing any settings. This was continued until each dosimeter was counted 4 times through 360 degrees. This was done to help account for the shielding effect of the bubbles. The upper and lower camera detection threshold settings as well as all 4 countings of the dosimeter were recorded on the original data sheets. The 4 countings were then averaged to yield an average number of bubbles for the dosimeter, and this value was used in all subsequent calculations. Standard deviations were also calculated. Appendix A contains all four readings of each dosimeter in each test as well as the standard deviation for each dosimeter.

2.4 Data Analysis

For each source used (AmLi and special sources 1 and 2), a graph of count rate versus straight line distance to the source was made. The experimental data is represented by points on each of these graphs. The software package Sciplot was used to draw the best fit line through these points. Sciplot takes pairs of x,y points representing distance and count rate and then calculates coefficients A, B, and C to fit the equation:

$$Y = A + \frac{B}{(X-R)} + \frac{C}{(X-R)^2} \qquad\qquad (2.1)$$

where: Y = Dosimeter Count Rate (bub/hr)

X = Distance from source (m)

R = Radius of the source (m)

If the source were a point source, the dosimeter count rate would fall off as $1/X^2$, while

if the source were a plane source it would decrease as $1/X$. By using both terms in the

equation, the source is being treated as both a point and a plane source. Subtracting the

radius (R) from the distance (X) takes into account the fact that the distances are measured

to the center of the object.

2.5 Background Determinations (Tests 2.1 and 2.2)

The first step in this research was to determine the background radiation in the

Accelerator Development Lab (ADL) and Kiva 2 since all experiments were to be

conducted in one of these two areas. Three BTI BD-100R dosimeters were placed

overnight in both the ADL and Kiva 2 to measure the background radiation in each area.

The background tests for the ADL and Kiva 2 were recorded as Tests 2.1 and 2.2

respectively. The temperature in each area was controlled and monitored by installed

thermostats to ensure the temperature in each area did not fall below 60 degrees Fahrenheit

throughout the entire irradiation time during the background measurement and all subsequent tests.

The three dosimeters from the ADL and the three from Kiva 2 were read using the bubble reader in Tech Area 55. Background radiation readings for the ADL and Kiva 2 were calculated as described in the test plan and bubble reader sections (2.2 and 2.3) and are contained in Appendices B and C respectively. The background radiation in the ADL was found to be 0.232 bubbles per hour while in Kiva 2 the background was considerably higher at 2.26 bubbles per hour due the presence of neutron sources within Kiva 2.

2.6 Americium Lithium (Test 2.5)

An Americium Lithium (AmLi) source of strength $4.9 * 10^5$ neutrons per second (n/sec) was obtained from Tech Area 18 and used to irradiate 27 BTI BD-100R devices in the ADL. The AmLi source was a small circular cylinder approximately 10 cm long and 4 cm in diameter connected to a carrying rod approximately 0.5 m long. This irradiation was recorded as Test 2.5.

The AmLi was chosen because it is a calibration source used for treaty verification applications due to its long half-life. Figure 2.1 shows the spatial distribution of the dosimeters used in this experiment with each position A - I representing three BTI dosimeters. A total of 3 radial distances from the source (0.25 m, 0.50 m, and 1.00 m)

were used with 9 dosimeters (3 groups of 3) at each distance. All dosimeters and the

AmLi source were positioned at approximately 1 meter above ground so they would be in

the same horizontal plane.

<figure>
Horizontal Spatial Distribution of BD-100R Dosimeters for Amli (Test 2.5)

AmLi Source
Strength = 4.9*10^5 n/sec

.25 m

.50 m

1.00 m

Count Rate Values for Dosimteters are Listed in Table 2.2
</figure>
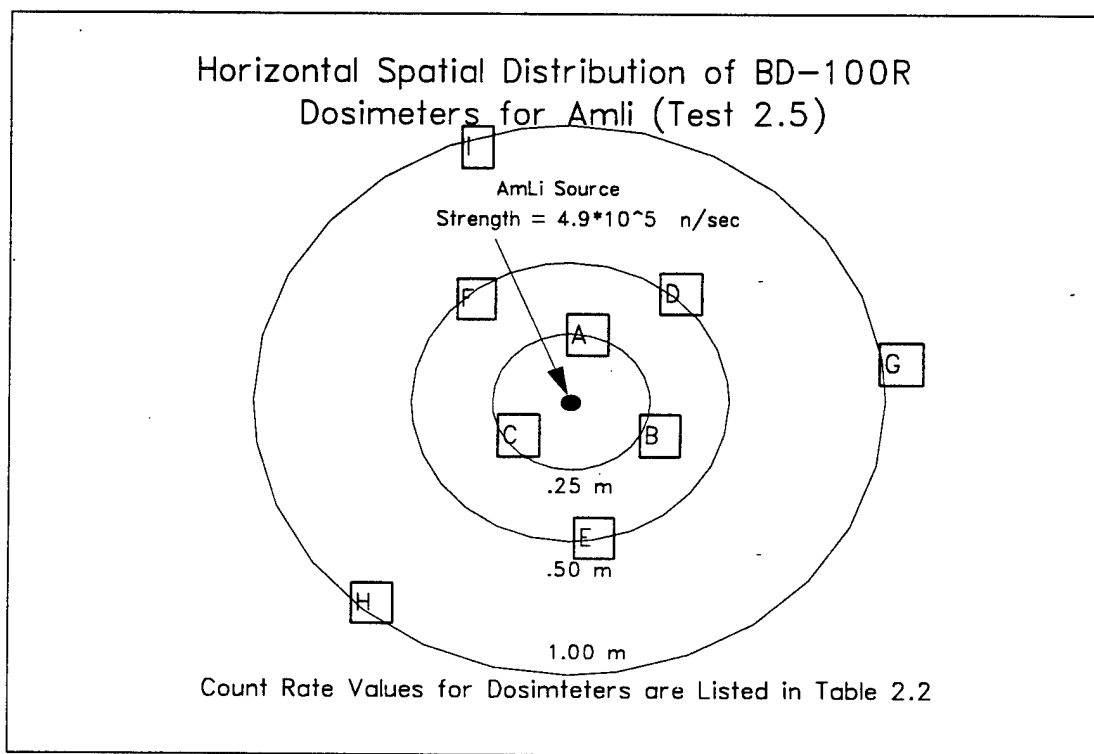
Figure 2.1 - AmLi Setup

The dosimeters from Test 2.5 were read using the bubble reader at Tech Area 55.

The count rates for the dosimeters were determined using the method discussed in the test

plan and bubble reader sections (2.2 and 2.3). These calculations are recorded in

Appendix B. The readings from each group of 3 dosimeters A - I were then averaged to

yield the average count rate produced by the source at each position. Table 2.2 lists the

27

average, maximum, and minimum count rates above background for each group
corresponding to Figure 2.1.

Table 2.2 - Spatial Response Above Background of BD-100R Dosimeters for AmLi
(Test 2.5)

Dosimeter Position	Avg Rate (bub/hr)	Max Rate (bub/hr)	Min Rate (bub/hr)
A	130	169	104
B	134	145	118
C	129	144	110
D	37.8	43.5	33.2
E	40.7	42.3	38.5
F	42.2	44.1	40.3
G	16.8	19.2	14.9
H	14.7	16.0	13.6
I	19.0	22.1	15.0

Dosimeter Sensitivity Normalized to 50 bub/mrem

Average Background Rate = 0.232 bub/hr

The groups of dosimeters at the same distance (A-C for 0.25 m, D-F for 0.50 m, and G-I for 1.00 m) were then averaged to yield an average count rate as a function of radial distance from the source. Figure 2.2 shows this data graphically. The points on this graph represent the average count rates at each distance and the plus and minus one standard deviation points. At 0.5 m and 1 m, these three points are close together and appear nearly as a single point. Standard deviation (σ) for the points was calculated using

the following equation:[18]

$$\sigma = \frac{\sqrt{\sum (Y_i - Y_{mean})^2}}{\sqrt{n-1}}$$

(2.2)

where Y_i = response of ith device

Y_{mean} = average response of devices at a given spatial position

n = number of observations
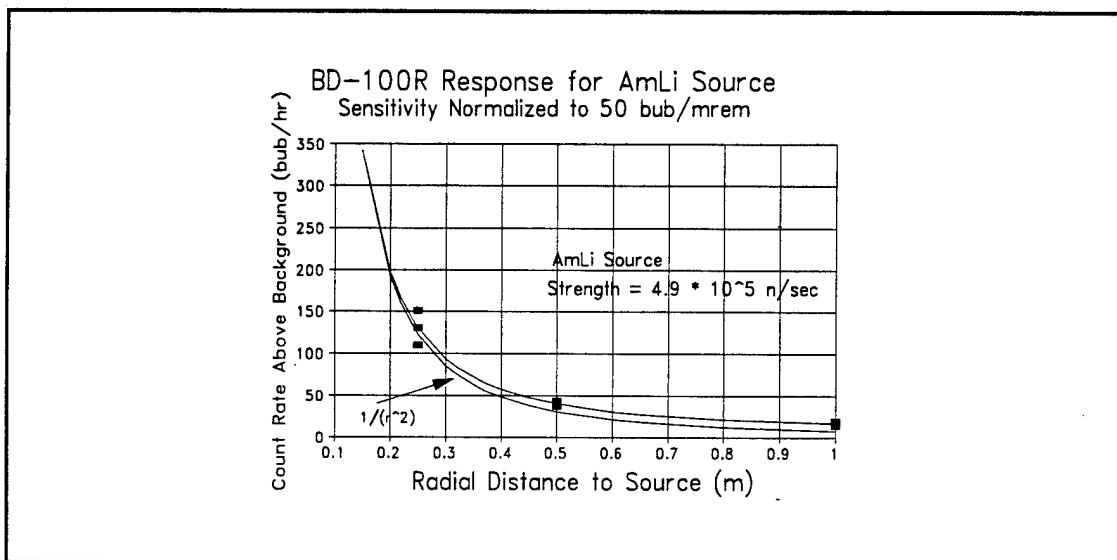
Figure 2.2 - AmLi Response

The curve through the data points is a best fit curve developed through a regression program (i.e. Sciplot) which is described in section 2.4, Data Analysis. For comparison, the inverse square law curve is also plotted.

29

2.7 Special Source 1 (Tests 2.6 and 2.7)

Special source 1 was approximately a circular cylinder lying horizontally on its shipping container. Other than special source 1 there were no neutron sources in the vicinity of the experiment. Test 2.6 was conducted overnight with 12 BTI BD-100R dosimeters (4 groups of dosimeters with 3 dosimeters per group) placed around special source 1. Test 2.7 was conducted for 5 hours and 40 minutes with 9 more BTI BD-100R devices, consisting of 3 groups of 3, placed around special source 1. For data analysis these two tests were combined since the same source was used. Figure 2.3 shows the spatial distribution of the dosimeters around special source 1 combining tests 2.6 and 2.7 with collocated positions A1 and A2 representing 3 dosimeters each, and positions B - F representing 3 dosimeters each. All dosimeters were positioned above ground so they would be in the same horizontal plane as the center of the special source.

The dosimeters from Tests 2.6 and 2.7 were read using the bubble reader at Tech Area 55. The count rates from special source 1 were calculated using the method described in the test plan and bubble reader sections. These calculations are recorded in Appendix C. Each group of dosimeters A - F was then averaged to give the average count rate for each group. Table 2.3 lists the average, maximum, and minimum count rates for each group of dosimeters corresponding to Figure 2.3.

Horizontal Spatial Distribution of BD-100R Dosimeters
for Special Source 1 (Test 2.6 and 2.7)

Count Rate Values for Dosimeters Are Listed in Table 2.3
All Distances Are Calculated to Geometric Center of Special Source
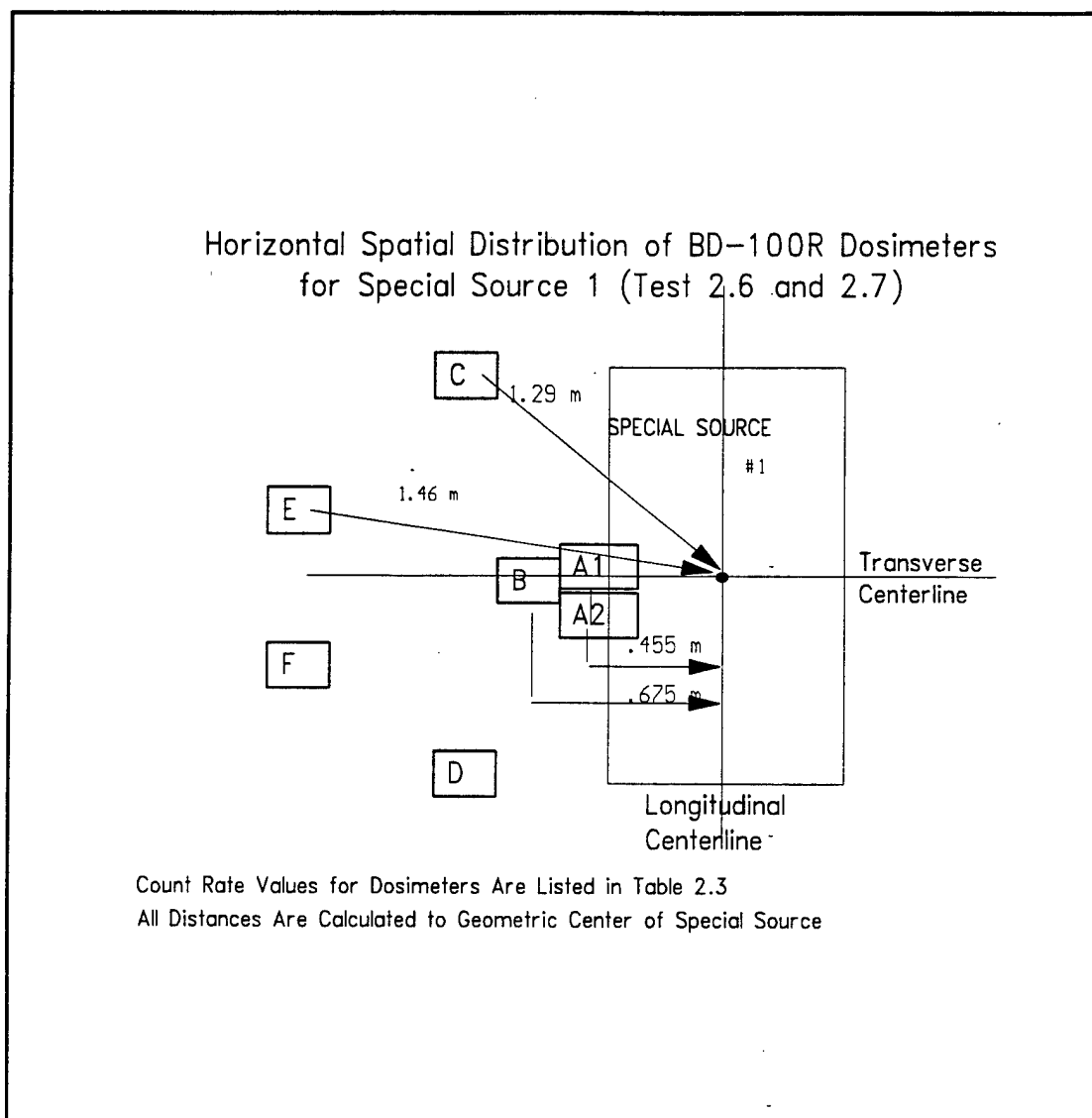
Figure 2.3 - Special Source 1 Setup

Each group of dosimeters has a corresponding distance as shown in Figure 2.3.

The distance from each group to the edge of the special source was measured, and then

the distance from each group to the center of the special source was calculated using right

triangles. The physical center of the special source was used as a reference for all

Table 2.3 - Spatial Response Above Background of BD-100R Dosimeters for Special Source 1 (Tests 2.6 and 2.7)

Dosimeter Position	Avg Rate (bub/hr)	Max Rate (bub/hr	Min Rate (bub/hr)
A1	19.2	22.6	14.9
A2	15.6	17.7	11.8
B	13.6	18.2	10.9
C	4.59	5.08	3.95
D	4.08	4.82	2.80
E	4.42	5.39	3.78
F	4.78	6.15	3.52

Dosimeter Sensitivity Normalized to 50 bub/mrem

Average Background Rate = 2.26 bub/hr

distances. The distance from the dosimeters to the center of the special source was considered negative if the dosimeter was positioned aft of the transverse centerline of the source and positive if forward of the transverse centerline. Dosimeter group A1 was positioned slightly forward of the transverse centerline and was therefore considered positive, whereas dosimeter group A2 was slightly aft of the transverse centerline and was considered negative. Because dosimeter group B consisted of 3 dosimeters and was positioned directly on the transverse centerline of the source, these dosimeters were considered as both positive and negative points. Figure 2.4 shows graphically the count rate as a function of the slant distance to the center of special source 1. The points on this graph represent the average count rates at each distance and the average values plus and minus one standard deviation. The standard deviation for these points was calculated

using Equation 2.2. The curves through the data points are best fit curves developed

through Sciplot.
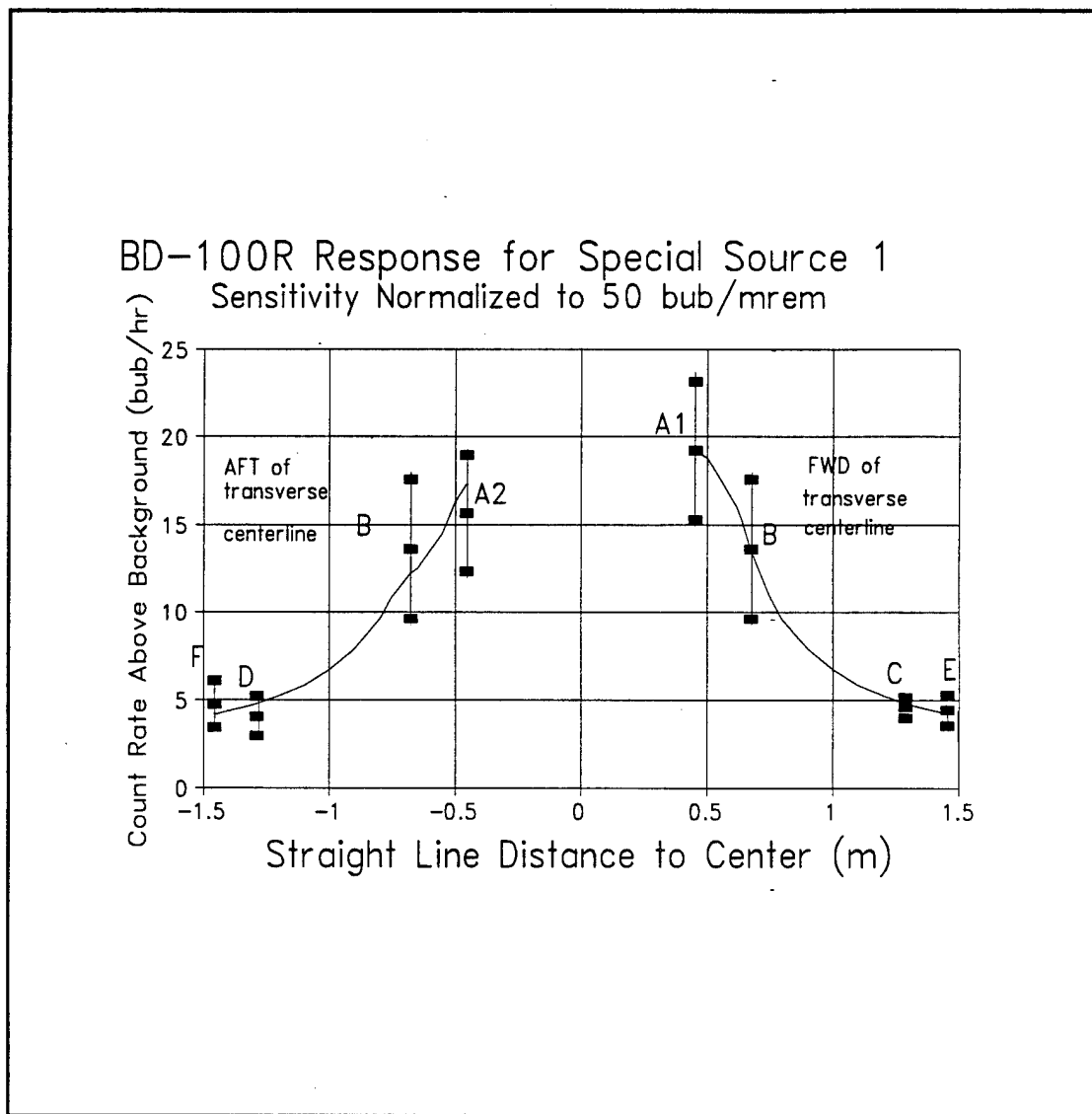
Figure 2.4 - Special Source 1 Response

Analysis of Figure 2.3 and Table 2.3 shows the ability of the BTI dosimeters to be used as a neutron mapping device that could be used to record a neutron signature for a given source. Because groups A1 and A2 are close together and that dosimeter group B represents both positive and negative distances, it can not be concluded for certain whether the neutron source in special source 1 lies on the transverse centerline or not. However, knowing the count rates at various positions around the source could be very helpful in distinguishing special source 1 from another source.

2.8 Special Source 2 (Tests 2.8 and 2.9)

Special source 2 was physically smaller than special source 1 and was approximately a circular cylinder lying horizontally on a wheeled dolly. No additional equipment or sources were present around special source 2 that were not present around special source 1. Test 2.8 was conducted for 3 hours and 50 minutes with 12 BTI BD-100R dosimeters taped individually to the edges of special source 2 at different locations. Test 2.9 was conducted overnight with 22 BTI BD-100R dosimeters in 4 groups of 3 and 5 groups of 2 placed around special source 2. Because 10 of the dosimeters were not in the same horizontal plane as the center of the special source, they were not used in data analysis. For data analysis these two tests were combined since the same source was used. Figure 2.5 shows the spatial distribution of the dosimeters used in Tests 2.8 and 2.9 around special source 2. A total of 24 dosimeters was used for analysis and were distributed as follows: positions A - D contained 2 dosimeters each (8 dosimeters), E - H contained 1 each (4 dosimeters), and I - L contained 3 each (12 dosimeters). All

34

dosimeters were positioned at a height above ground to correspond to the horizontal center

of the special source.

Horizontal Spatial Distribution of BD-100R Dosimeters
for Special Souce 2 (Test 2.8 and 2.9)

Count Rate Values for Dosimeters Are Listed in Table 2.4
All Distances Are Calculated to Geometric Center of Special Source
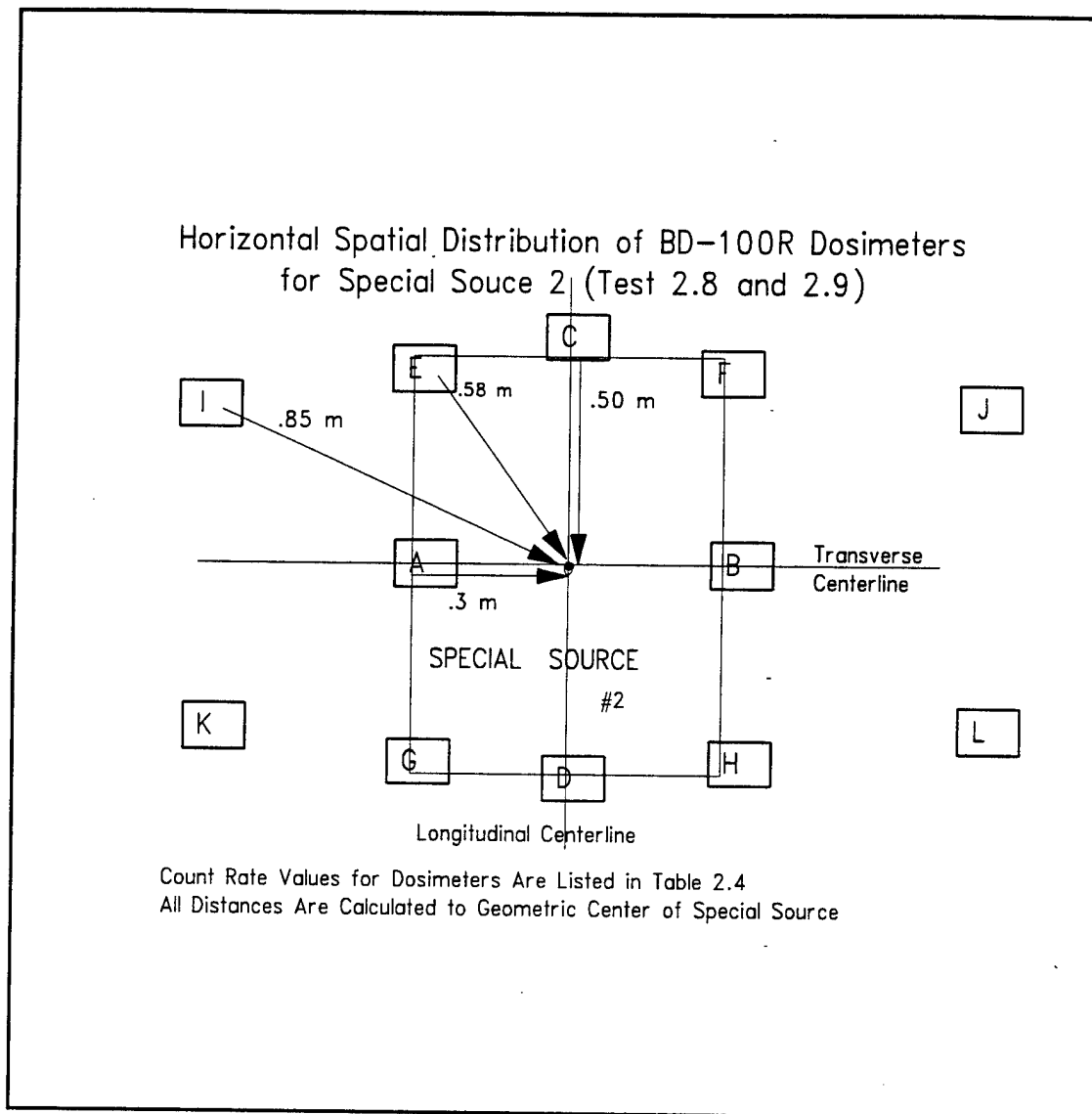
Figure 2.5 - Special Source 2 Setup

The dosimeters from Tests 2.8 and 2.9 were read using the bubble reader at Tech Area 55. The count rates from special source 2 were calculated as described in the test plan and bubble reader sections. These calculations are recorded in Appendix D. Table 2.4 lists the average, maximum, and minimum count rates for each dosimeter position A - L corresponding to Figure 2.5.

Table 2.4 - Spatial Response Above Background of BD-100R Dosimeters for Special Source 2 (Tests 2.8 and 2.9)

Dosimeter Position	Avg Rate (bub/hr)	Max Rate (bub/hr)	Min Rate (bub/hr)
A	22.9	23.0	22.8
B	27.7	30.7	24.7
C	8.74	9.78	7.69
D	1.71	1.83	1.60
E	6.28	*	*
F	5.92	*	*
G	0.62	*	*
H	2.32	*	*
I	2.82	3.17	2.18
J	3.77	4.54	2.86
K	2.85	4.13	2.06
L	2.19	2.97	1.28

* - N/A Because Only 1 Dosimeter

Dosimeter Sensitivity Normalized to 50 bub/mrem

Average Background Rate = 2.26 bub/hr

As with special source 1, each dosimeter around special source 2 has a corresponding distance as shown in Figure 2.5. All distances were measured to the edge of the source and then calculated to the center of the source. The same sign convention used for special source 1 was used for special source 2. Because both dosimeter groups A and B were positioned on the transverse centerline, they were averaged together and were considered as both positive and negative points. Figure 2.6 shows graphically the count rate as a function of the slant line distance from the center of special source 2. Because groups E and F are at the same distance from the center, they plot as one point on the graph. The same is true for groups I and J, G and H, and K and L. The points on this graph represent the average count rates at each distance and the average values plus

BD-100R Response for Special Source 2
Sensitivity Normalized to 50 bub/mrem
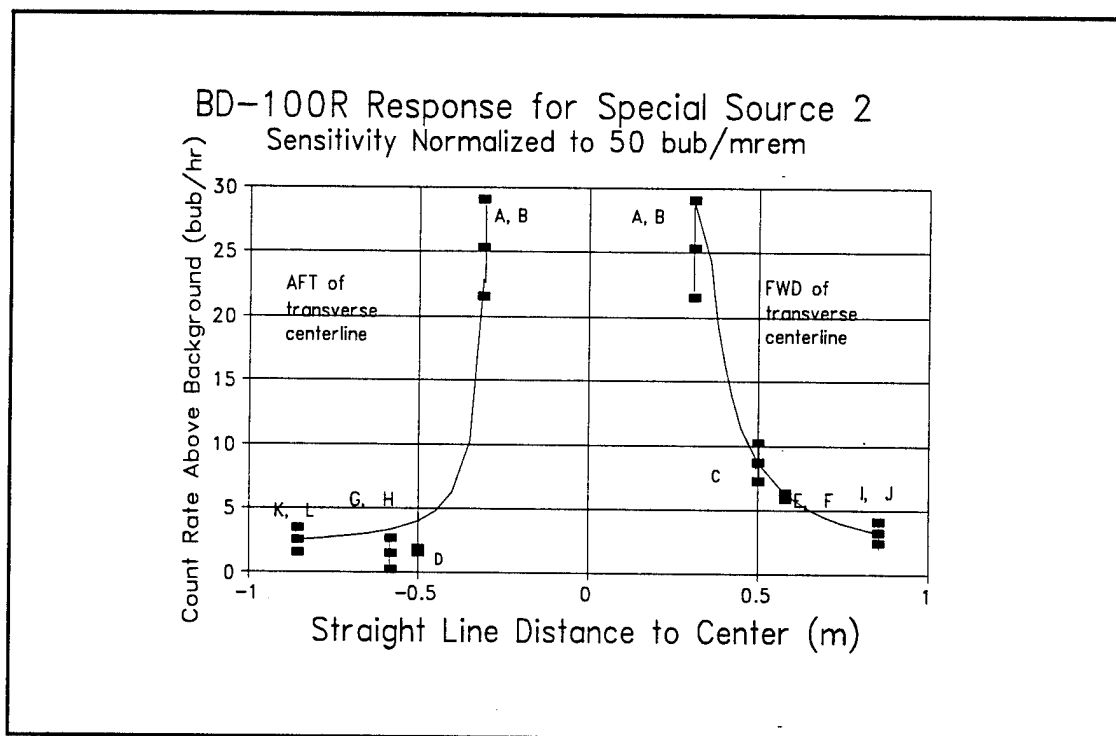
Figure 2.6 - Special Source 2 Response

and minus one standard deviation. For groups A-B and groups of 3 dosimeters (I, J, K, and L) the standard deviation was calculated using equation 2.2. For groups of 2 dosimeters (C, D, E-F, and G-H), σ was calculated using the equation:[18]

$$\sigma = \sqrt{Y_{mean}} \qquad\qquad (2.3)$$

The curves through the data points are best fit curves developed by Sciplot.

As with special source 1, the neutron mapping capability of the BTI dosimeters is evident in Figure 2.5 and Table 2.4 for special source 2. By analyzing pairs of dosimeter groups such as C and D, E and G, and F and H it can be concluded that the neutron source within special source 2 is probably not in the physical center of the source, but rather may lie forward of the transverse centerline. By using all the dosimeter groups together, a neutron signature can be obtained for special source 2 that could be used to differentiate it from another source.

2.9 Source Comparisons

Table 2.5 is a comparison of bubble count rates from different sources. This data shows that a smaller bubble count rate can be expected from a special source due to the smaller strength of the special source in comparison to that of the AmLi source used. From past research as well as research detailed in Chapter V, the bubble dosimeter response is independent of neutron energy within the fission energy spectrum (approximately 1 to 2.5 MeV).[1]

Table 2.5 - Comparison of Bubble Count Rates for Different Sources

Source	Distance (m)	Count Rate (bub/hr)	Reference
AmLi	0.25	131	(1)
Special Source 1	0.3	17.4	(2)
Special Source 2	0.3	25.3	(3)

Distances measured to geometric center of the source.

(1) Appendix B, average of groups A, B, and C
(2) Appendix C, average of groups A1 and A2
(3) Appendix D, average of groups A and B

This fact is supported by the data regarding the AmLi test. Even though the AmLi source emits low energy neutrons it gave a much higher bubble count rate due to the fact that it emits more neutrons than the special sources. This data also shows the importance of testing the bubble dosimeters around sources that closely resemble those that would be found in treaty verification applications rather than just with point neutron sources such as AmLi or Cf^{252}.

2.10 Graphical Analysis

As mentioned in the Data Analysis section, the curves for Figures 2.2, 2.4, and 2.6 are best fit curves developed by Sciplot. Table 2.6 lists the coefficients A, B, and C for each curve calculated by Sciplot. Analysis of Table 2.6 can lead to conclusions about the behavior of the different sources. Due to the size and shape of the AmLi source, it would be expected to act like a point source. This was found to be the case due to the large

value of its C coefficient as shown in Table 2.6. Because of the size and distribution of source material within the special sources, it would be expected that neither would act like a point source. This was found to be the case as evidenced by the fact that the magnitude of the B coefficients were much greater than the C coefficients for both special sources as shown in Table 2.6. A better description of the special sources would be as spherical volumetric sources.

Table 2.6 - Coefficients for Graphs of Count Rate versus Distance

Cases	A	B	C
AmLi	8.10	1.41	7.32
Special Source 1 -	0.765	3.57	-0.0937
Special Source 1 +	0.853	3.54	-0.0896
Special Source 2 -	1.67	.483	-0.0027
Special Source 2 +	0.0319	1.80	-0.0152

Coefficients fit the Equation:

$$Y = A + B/(X-R) + C/(X-R)^2$$

Where: Y = Count Rate (bub/hr)
          X = Slant Distance from source (m)
          R = Radius of Source (m)

2.11 Device Response Uncertainty

An important factor in determining the requirements for using the bubble dosimeter as a neutron detector for treaty verification is the coefficient of variation associated with the reading. It is important that the bubble dosimeter produces enough counts to yield a statistically significant reading. It has been proven in past research that the response of the bubble dosimeters can be described by Poisson statistics.[1] Using this fact, the coefficient of variation, representing the uncertainty associated with a certain number of observations, can be calculated by the following equation:[18]

$$Coefficient.of.Variation = \frac{1}{\sqrt{Y_{mean}}} \qquad (2.4)$$

where Y_{mean} = average number of counts

For example, a dosimeter containing a mean of 100 bubbles has a coefficient of variation (percent uncertainty) of 0.10 or 10% while a dosimeter containing 10,000 bubbles has a coefficient of variation of 1%. Equation 2.4 can be used to find the mean number of bubbles necessary to produce a specified coefficient of variation. Using this technique and the count rates established from the special sources, the irradiation time can be determined to give a specified coefficient of variation for each source. One method to decrease the required irradiation time for a given coefficient of variation is to increase the number of detectors used, thus increasing the number of counts (Y) recorded throughout the irradiation. Because of their small size and ease of use, the BTI BD-100R dosimeters are easily used in groups as demonstrated in these experiments. This approach was used to

41

calculate the time required to achieve a given coefficient of variation (1-10%) with a given number of dosimeters (1, 5, 10, 20, and 50) using the highest average count rate for each individual source (17.4 bub/hr for special source 1 and 25.3 bub/hr for special source 2). Results are tabulated in Appendix E. Figures 2.7 and 2.8 are graphs of irradiation time versus coefficient of variation for special sources 1 and 2 respectively, each having a family of curves that represent the number of BTI dosimeters required to achieve the desired uncertainty.

Another possible approach to solve this problem is to increase greatly the sensitivity of the bubble dosimeters. Increasing the sensitivity of each device by a factor of 10, from 50 bubbles per mrem to 500 bubbles per mrem, would create the same reduction in the coefficient of variation as would using 10 normal BTI dosimeters. A combination of increasing the sensitivity of the dosimeters and using multiple dosimeters would be very effective in decreasing the uncertainty associated with the bubble dosimeters. The possibility of greatly increasing the sensitivity of the BTI dosimeters is currently being studied.[19]
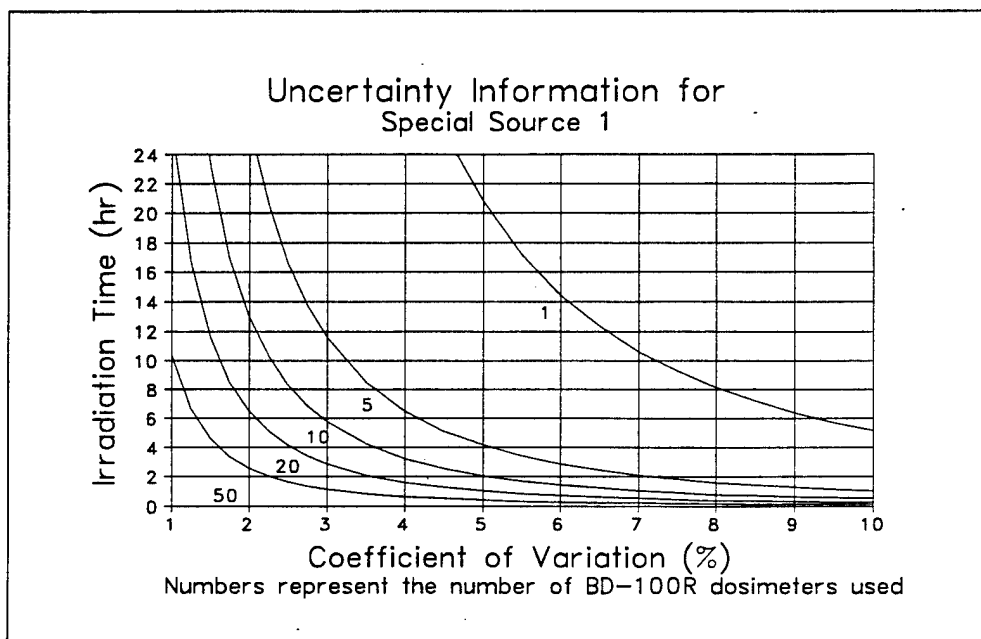
Figure 2.7 - Uncertainty Information for Special Source 1
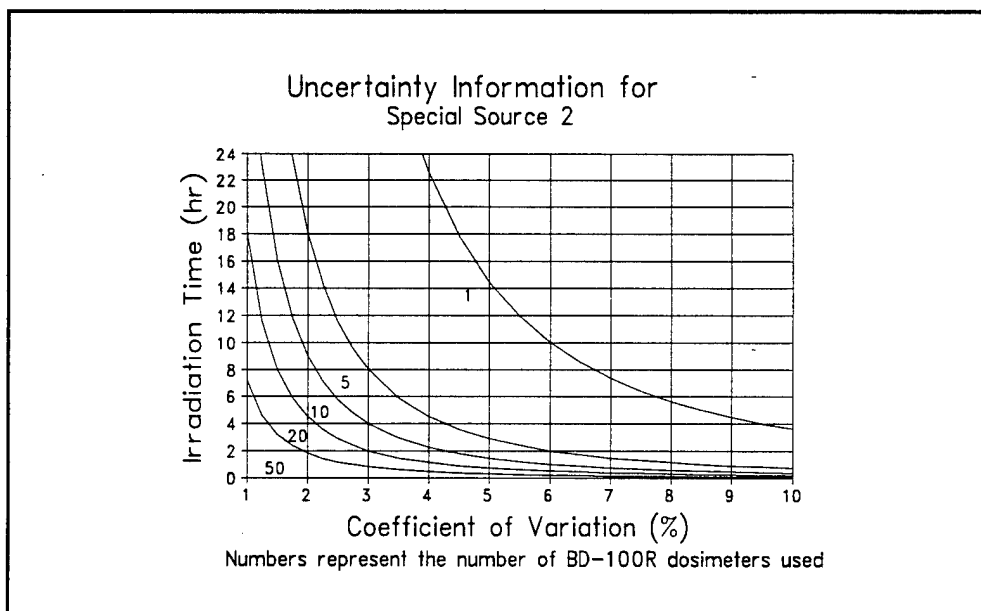
Figure 2.8 - Uncertainty Information for Special Source 2

2.12 Sensitivity Comparisons

During the AmLi experiment (Test 2.5), an additional neutron detector, the NNV-470 obtained from Tech Area 18, was used to provide a comparison for the BTI dosimeters. The NNV-470 is an enriched lithium iodide scintillator that converts gamma and neutron radiation into light signals and then into pulses of electrical current. The NNV-470 is able to discriminate between neutron and gamma radiation since the amplitude of the neutron pulses is much greater than that of the gamma pulses.

Table 2.7 - Comparison of Sensitivity of NNV-470 versus Sensitivity of BD-100R

Radial Distance (m)	Counts Using NNV (cts/sec)	Counts Using BD-100R (cts/sec)	Relative Sensitivity
0.25	28.9	0.0363	795
0.50	10.4	0.0112	929
1.00	3.99	0.0047	854

Source used was AmLi (Test 2.5)

Mean Value of all BD-100R readings normalized to 50 bubbles/mrem

Relative Sensitivity is the sensitivity of NNV compared to BD-100R

The NNV-470 is more sensitive to thermal neutrons than fast neutrons, and records counts over a 20 second interval. The NNV-470 was placed at the same 3 distances from the source as the BTI dosimeters, 0.25 m, 0.50 m, and 1.00 m. The data for the NNV-470 is contained in Appendix B. Table 2.7 lists the counts per second from both detectors as well as the relative sensitivity of the NNV-470 compared to the BTI dosimeters at 3

distances. As can be seen from Table 2.7 the NNV-470 has a sensitivity of approximately 850 times that of a single BTI BD-100R dosimeter.

2.13 Conclusions

By analyzing the data obtained from this research, several conclusions can be drawn with regard to using bubble dosimeters for neutron detection and treaty verification. From Figure 2.2, it is apparent that the count rate recorded by the bubble dosimeters approximates the $1/r^2$ rule. Due to this fact, dosimeters at 0.5 meter from the source required in excess of 20 hours to create 100-200 bubbles for special sources. Because of this, it is clear that the dosimeters must be placed close to, i.e. on contact with, a special source. Also from this data it can be concluded that possible ways around this problem include using very highly sensitive dosimeters and/or multiple (>10) dosimeters.

This research also shows that the BTI dosimeters could be used to map a given special source to identify the source based on the spatial response of the dosimeters. The BTI dosimeter's small size makes it a better point detector than large detectors that record counts from a large area. Because of this, several BTI dosimeters can be placed around a source, irradiated concurrently, and read to yield count rates on many points around a source. Using the data in this report, it would be possible to differentiate between special sources 1 and 2 based solely on the ratio of the count rates from dosimeters at various positions around the source. A more detailed intensity profile could be obtained by placing the dosimeters in a 360 degree ring around the source rather than just in one horizontal plane. Detailed mapping of a source would greatly increase the ability to

identify a source based solely on the relative count readings taken from different areas on the source.

Chapter III

Gamma Sensitivity Tests

The relevance and expectations of a bubble dosimeter's gamma sensitivity are explained. The setup and results for each detector are given. Conclusions on the gamma sensitivity of each detector are drawn.

3.1 Background

The nuclear material present in nuclear munitions can be expected to produce a mixed radiation field of neutron and gamma radiation due to the presence of plutonium and/or highly enriched uranium. Because of the obtrusiveness of gamma spectrum analysis, it is important that the detector's neutron response be independent of the gamma field present.

In the study of bubble dosimeters, both Harper and Rich calculated the critical energy required to form a bubble (E_c) and denoted the energy deposited by a recoil ion as E_a.[1,10] Harper determined that if a recoil ion was able to deposit E_a in a given distance within the bubble material, then bubble nucleation would occur.[10] Since the stopping power of the bubble material is higher for neutrons than gamma rays, incident gamma rays were assumed to be unable to deposit E_a in the required distance and, therefore, would be unable to cause nucleation.

3.2 Experimental Setup

The objective of this research was to determine the gamma sensitivity of the BTI BD-100R, the Apfel R-12 SDD, the Apfel HFC SDD, and the Apfel HFP SDD at varying gamma doses and varying degrees of reuse. All irradiations for this experiment were conducted at AFRRI in Bethesda, Md. The sequences of radiation exposure are shown in Table 3.1.

Table 3.1 - Summary of Groups for Gamma Sensitivity Tests

Gamma Sensitivity Studies: (Both Apfel and BTI)

Group 1:
      G -> G -> G   (G = 50 Rads Gamma Radiation)
Group 2:
      G -> G -> G   (G = 500 Rads Gamma Radiation)
Group 3:
      G -> G -> G   (G = 5000 Rads Gamma Radiation)

Reuse Studies: (BTI dosimeters only)

      G = 5000 Rads Gamma Radiation
      N = Neutron Exposure
      R = Repressurization

Group 4:
      N -> G -> N -> G -> N -> G
Group 5:
      N -> N -> N-> G
Group 6:
      N -> R -> G -> N -> R -> G -> N -> R -> G
Group 7:
      N -> R -> N -> R -> N -> R -> G
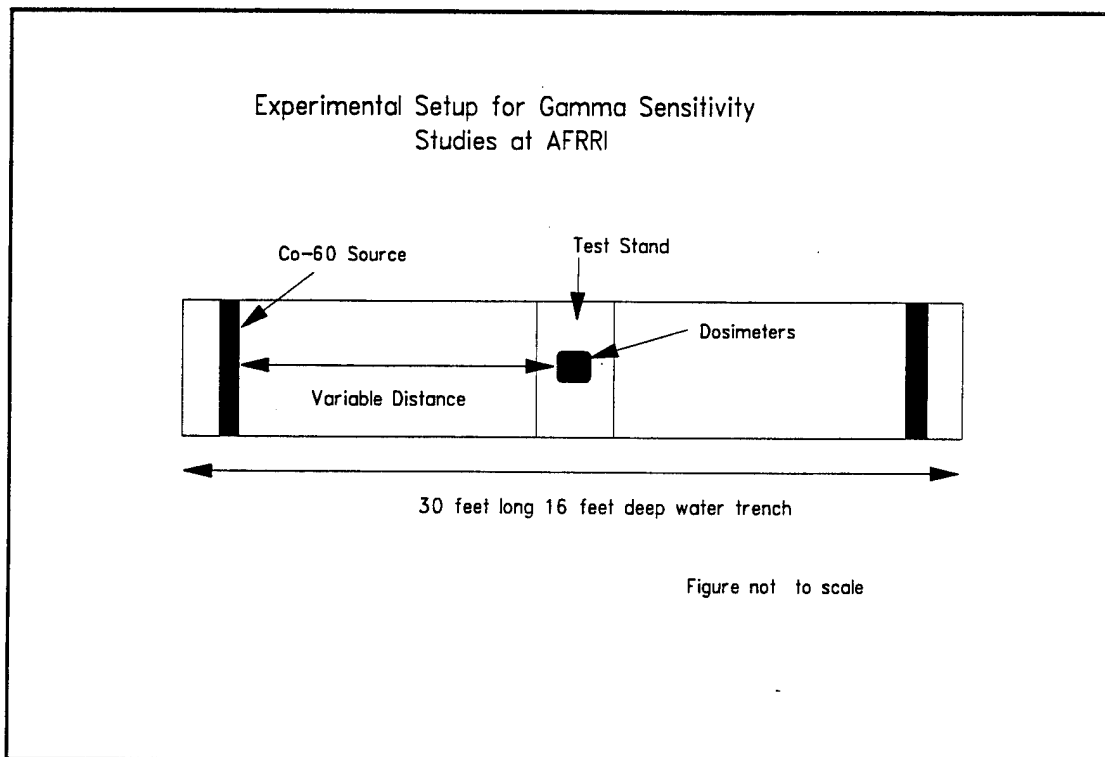
Figure 3.1 - Gamma Studies Setup

Gamma irradiations were conducted with Co^{60} sources. The Co^{60} facility at AFRRI

consists of 2 groups of 8 Co^{60} elements that are contained in opposite ends of a 16 feet

deep trench of water with a test table located at the top middle section of the trench. The

dosimeters were placed on the test table, and the Co^{60} elements were raised on two

separate elevators for the duration of the tests. Figure 3.1 shows the experimental setup

used at AFRRI for all gamma irradiations. The number of elements, irradiation time, and

distance between the dosimeters and elements were all determined by AFRRI personnel

for each test to give the desired gamma dose. This dose calculation included an integration

to account for the rise and fall of the sources. This setup was deemed sufficient since the

49

only variable to be studied was the total dose delivered to the dosimeters.

All neutron irradiations were also conducted by AFRRI personnel using a PuBe source for approximately 8 minutes to produce a readable number of bubbles (<300). This procedure was sufficient since no quantitative estimate of the device's neutron sensitivity was to be derived from these irradiations. The only purpose of the neutron irradiations was to determine if the dosimeters became gamma sensitive after repeated neutron irradiations.

To determine the effect of gamma dose, all dosimeters were irradiated at gamma dose levels of 50, 500, and 5000 rads. To determine the effect of reuse, the BTI dosimeters were intermixed with neutron irradiations, gamma irradiations, and repressurizations of the dosimeter as shown in Table 3.1. Due to an unexpected failure of both ASM's, reuse studies of the Apfel devices were not possible.

The Apfel dosimeters and the two ASM's were initially irradiated to determine quantitatively the response due to gamma radiation. Unfortunately when the ASM's received the 5000 rad exposure, both became inoperative. Both ASM's were sent back to Apfel for repair. Apfel responded that the high gamma dose caused failure of the circuitry within the ASM.[20] Following failure of the ASM's, the Apfel dosimeters were irradiated in their vials alone. This was possible since any response in the vials would cause visible bubbles (similar to the BTI dosimeters except that in the Apfel vials the bubbles would rise out of the gel). This approach allowed for only qualitative determination of the Apfel dosimeters' gamma sensitivity.

3.3 Experimental Results

The BTI dosimeters were arranged into 7 groups of 5 dosimeters each with each group having a different irradiation history. The irradiation history and the average number of bubbles present at each stage are listed in Appendix F. From Appendix F it can be seen that no bubbles were formed in any of the dosimeters in groups 1-3. In groups involving neutron irradiations, the only value of concern is the change in number of bubbles present following a gamma radiation. For example, in group 4, following the 3 gamma irradiations there was an apparent change of 3, 5, and -3 bubbles respectively. The small changes, including the negative value, can easily be attributed to inaccuracies of the bubble reader and not to any actual response to gamma radiation. Similar results are found for Group 5. Groups 6 and 7 showed zero effect of gamma radiation.

Results for the Apfel R-12 dosimeter were obtained by visually inspecting the vials after irradiation. No bubbles were observed in any of the gamma irradiation tests over the three dose levels. Similar results were obtained for the Apfel HFC dosimeter for the same irradiations. However, after 50 rads total dose the HFP vial had several (approximately 100) bubbles which caused the gel material to overflow from the vial. A significantly greater number of bubbles was also observed when the HFP vials were subjected to 500 and 5000 rads. At 5000 rads the HFP vials were almost completely empty of droplet material.

3.4 Conclusions

From the data taken in this experiment, it is possible to make qualitative determinations on the gamma sensitivity of the various bubble dosimeters. Based on the presence or absence of bubbles, the gamma sensitivity of each dosimeter can be determined. Table 3.2 lists each dosimeter and whether it is gamma sensitive at each gamma dose level.

Table 3.2 - Summary of Gamma Sensitivity Tests Using Co^{60} Gamma Source

Detector	Is Detector Gamma Sensitive After:			
	50 Rads	500 Rads	5000 Rads	Reuse
BD-100R	No	No	No	No
Apfel R-12	No	No	No	*
Apfel HFC	No	No	No	*
Apfel HFP	Yes	Yes	Yes	*
ASM	No	No	Yes**	*

* - Due to failure of ASM at high gamma doses, reuse studies
of Apfel dosimeters were not possible

** - ASM failure occurred at 5000 Rads

No significant increase in the number of bubbles was ever observed immediately following any gamma irradiation for the BD-100R, the Apfel R-12, or the Apfel HFC. Based on these findings it was concluded that these dosimeters are not gamma sensitive. Additionally, from data taken after varying neutron exposures, it was concluded that the BD-100R remains gamma insensitive after reuse. Therefore, the BD-100R, the Apfel R-12, and the Apfel HFC can not be ruled out as candidates for treaty verification applications based on gamma sensitivity.

Because bubbles were observed in the Apfel HFP after gamma irradiation, it was concluded that the HFP is gamma sensitive, and therefore is not suitable for treaty verification applications. Additionally, it should be noted that the ASM failed at 5000 rads and therefore should not be exposed to these levels of gamma radiation.

Chapter IV

Temperature Response Studies

The objective, experimental setup, and experimental results of the temperature response studies are detailed. The theoretical response of the HFC compound is reinvestigated. Conclusions are drawn on the temperature response of the HFC and R-12 dosimeters.

4.1 Background and Objective

One of the predominant problems associated with using the bubble dosimeter for arms control verification applications is the bubble dosimeter's changing response with variations in temperature. It is desired that any arms control verification device give a constant response with changing temperature. This would allow the device to be used in a field environment rather than in a temperature controlled environment. As mentioned previously, BTI and Apfel's attempts to correct for temperature are limited since the BTI temperature compensating fluid has a limited range and the Apfel computer algorithm assumes a given neutron source energy. Rich's approach was to find a droplet material that would give a constant response within a useful temperature band. Based on Rich's conclusions it was predicted that the HFC SDD would give a constant response between 25 and 45 degrees Celsius.[1] Research by Rich, Harper, and Apfel concluded that the response of the R-12 dosimeter increases with increasing temperature.[1,10,20]

For economic reasons, Apfel was chosen over BTI to investigate the alternate materials researched by Rich. Research by Apfel concluded that only HFC and HFP were

stable in the SDD gel matrix.[20] Based on the results from the gamma sensitivity tests, HFP was dropped as a candidate for arms control verification which left only HFC as a possible candidate. Therefore it was the objective of this research to determine the response of the HFC as a function of temperature. In addition the temperature response of the R-12 dosimeter was measured for comparison purposes.

4.2 Experimental Setup

The temperature response studies were conducted at USNA using an unmoderated Cf^{252} neutron source and a low temperature incubator. Figure 4.1 shows the experimental setup used for the temperature response studies. In this experiment, 2 ASM's, one containing an HFC SDD, the other an R-12 SDD, were placed inside the incubator with the Cf^{252} source placed outside the incubator directly above the dosimeters. The positions of the source and dosimeters were marked to allow for a repeatable procedure. Each irradiation was conducted for 8 minutes. The temperature of the incubator, the only variable in the experiment, was set and monitored with an installed thermostat. The thermostat was checked using a separate digital thermocouple and proved to be accurate within 1 degree Celsius.
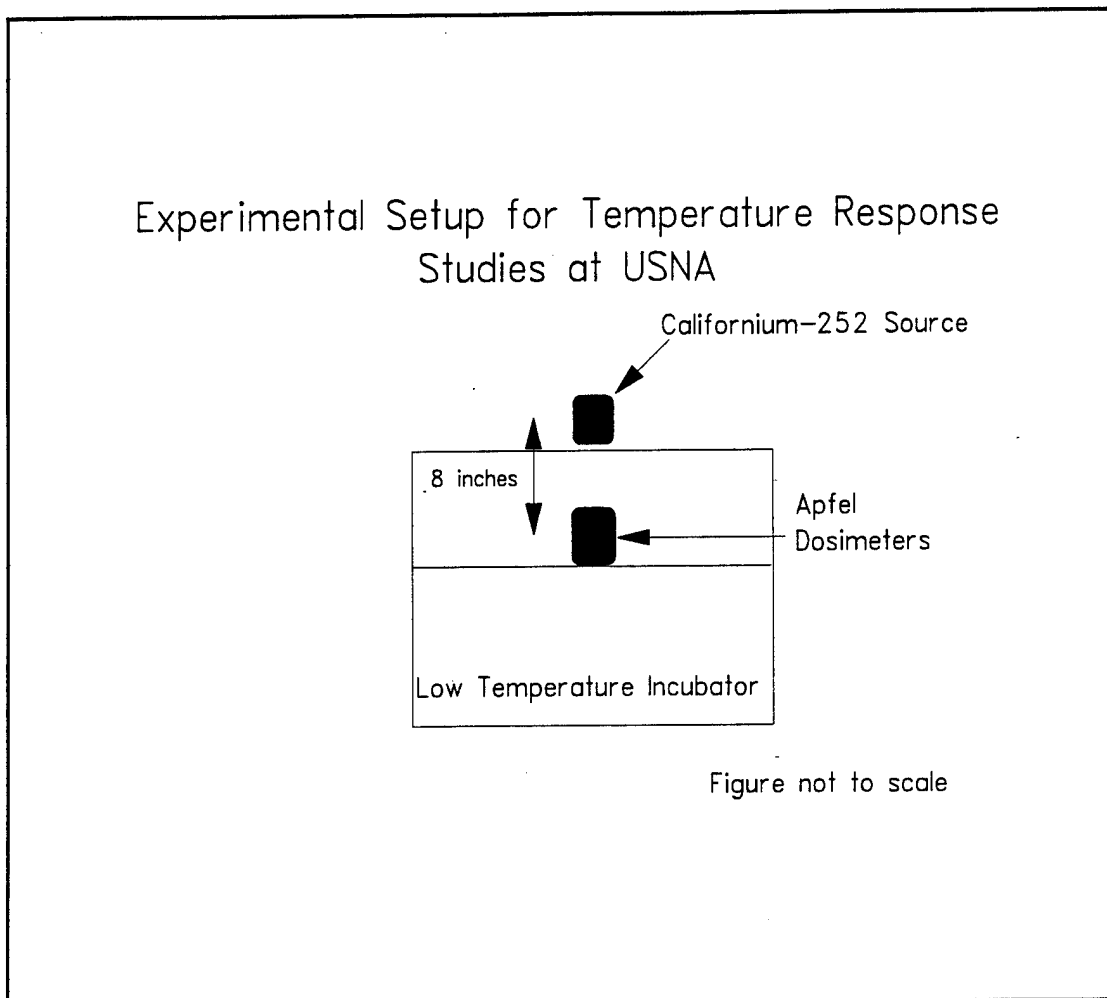
Figure 4.1 - Temperature Studies Setup

The response of the HFC SDD was studied at 13 different temperatures from 0 to 50 degrees Celsius. The HFC SDD was irradiated three times at each temperature (a total of 39 irradiations) to obtain an average response at each temperature. Due to failure of one ASM, the response of the R-12 SDD was studied at only 9 different temperatures. Like HFC, the R-12 SDD was irradiated three times at each temperature (a total of 27 irradiations) to obtain an average response at each temperature. A fresh SDD (both HFC

and R-12) was used at each new temperature to avoid excessive corrections for droplet depletion.

During the experiments it was determined that more time was required for the dosimeters to reach thermal equilibrium at lower temperatures than for higher temperatures. This was observed by the fact that the response for lower temperatures decreased as equilibration time was increased. Because of this, the dosimeters were allowed to equilibrate in the incubator overnight for temperatures < 20 degrees Celsius and for a minimum of 4 hours for temperatures > 20 degrees Celsius. During this equilibration time, the Cf^{252} source was placed in its shielding container away from the dosimeters. Background measurements were determined to be < 0.2 mrem per hour with an AN-PDR 70 neutron rem-meter. Since there was some background radiation, the dosimeters were left active during this equilibration time so that the number of pops from background could be recorded.

4. 3 Experimental Results

Appendix G contains all raw and calculated data for both the HFC and R-12 dosimeters. For each irradiation, the temperature from the installed thermostat, raw number of pops from the dosimeter (P_{raw}), and the total on-time for the ASM (T_{ASM}) were recorded. Because the sensitivity of both SDD's is a function of the number of droplets within the SDD, a count of the number of droplets within each SDD was maintained assuming each SDD had 24,000 droplets initially. This was accomplished by subtracting the number of pops during the equilibration time from 24,000 and then subtracting from

57

this result the number of pops for each subsequent irradiation.

Because the total number of pops for an individual SDD was significant over the duration of the three irradiation exposures, a sensitivity correction factor (CF_{sens}) was calculated based on the initial number of droplets ($D_{initial}$) and the final number of droplets (D_{final}) for an individual irradiation. Assuming a linear relation between detector sensitivity and number of droplets, and that the average number of droplets present for the duration of any given irradiation is $D_{initial} - 0.5*(D_{initial} - D_{final})$, the CF_{sens} was calculated using the following equation:

$$CF_{sens} = \frac{24000}{D_{initial} - 0.5*(D_{initial} - D_{final})} \qquad (4.1)$$

The purpose of the CF_{sens} was to correct the detector sensitivity for the depletion of droplets. The largest CF_{sens} ever calculated was 1.241 for HFC at 45 degrees Celsius which corresponded to a D_{final} of 18,889.

It was desired for each irradiation to last for 8 minutes (480 seconds). Ten seconds were allocated to allow for placement and removal of the dosimeters and source, which brought the total active time for the dosimeters to 490 seconds. Due to slight differences in exactly when the dosimeters were turned on/off, T_{ASM}'s ranged from 470 to 530 seconds. To compensate for this a time correction factor (CF_{time}) was developed to normalize all data to 490 seconds. The CF_{time} was calculated using the following equation:

$$CF_{time} = \frac{490}{T_{ASM}} \qquad (4.2)$$

The calculated CF_{time}'s ranged from 0.916 to 1.030 with most values being close to 1.000.

58

For each irradiation a corrected number of pops (P_{cor}) was found by the equation:

$$P_{cor} = CF_{sens} * CF_{time} * P_{raw} \qquad (4.3)$$

The P_{cor}'s for the 3 irradiations at each temperature were then averaged to yield a sensitivity and time corrected average number of pops for both dosimeters at each temperature. Figures 4.2 and 4.3 show the temperature response of HFC and R-12 respectively. Figures 4.4 and 4.5 show this same response with all values normalized to the response of the respective dosimeter at 25 degrees Celsius. Figures 4.2 - 4.5 show that both dosimeters have an increasing response with increasing temperature from 0 to 50 for HFC and 0 to 40 degrees for R-12. Additionally, analysis of Figures 4.4 and 4.5 shows that there is a temperature region for each dosimeter where the response is nearly linear with increasing temperature. This region is 20 to 40 degrees Celsius for HFC and 10 to 40 degrees Celsius for R-12. By performing a linear regression on the points in this linear region for each dosimeter, a temperature correction factor (TCF) can be generated for the devices. The TCF relates the response for any temperature in the linear region to the response of the dosimeter at 25 degrees Celsius. Figures 4.6 and 4.7 show the TCF as a function of temperature for HFC from 20 to 40 degrees Celsius and R-12 from 10 to 40 degrees Celsius respectively.
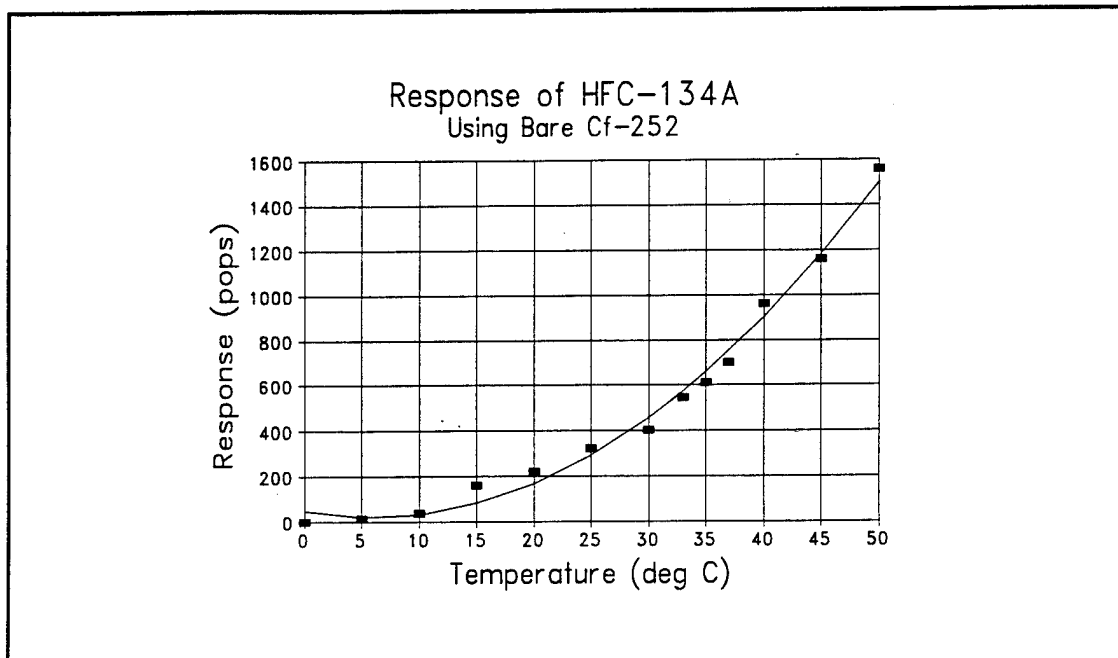
Figure 4.2 - Raw Response of HFC Versus Temperature
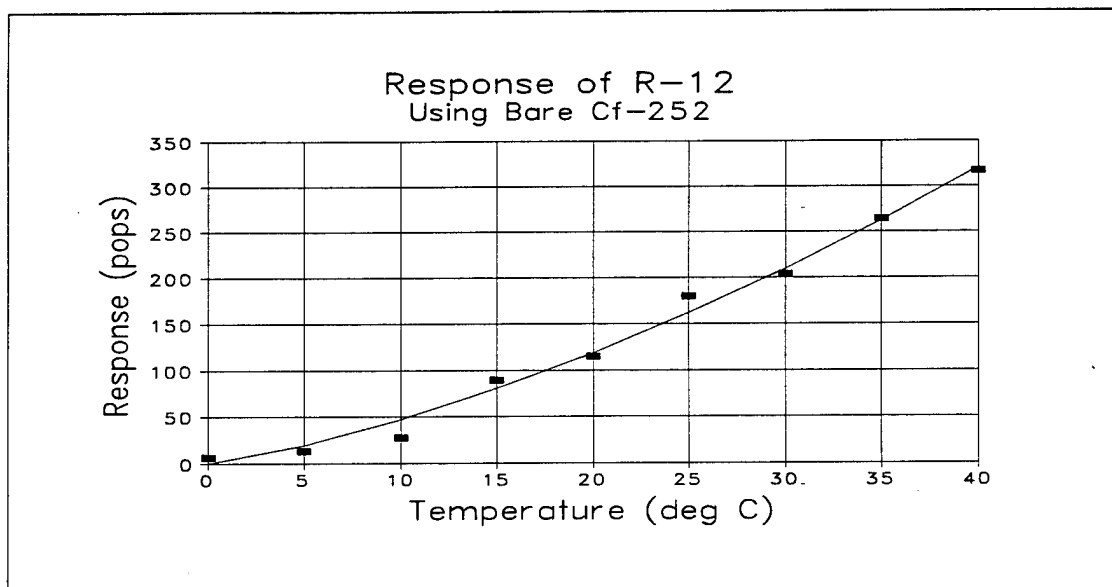
Figure 4.3 - Raw Response of R-12 Versus Temperature
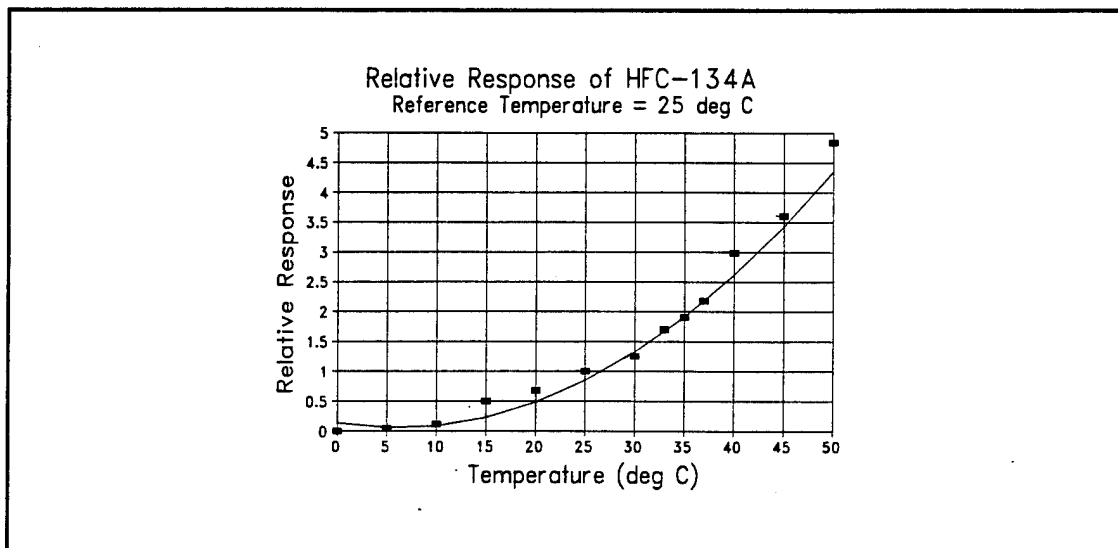
Figure 4.4 - Relative Response of HFC Versus Temperature
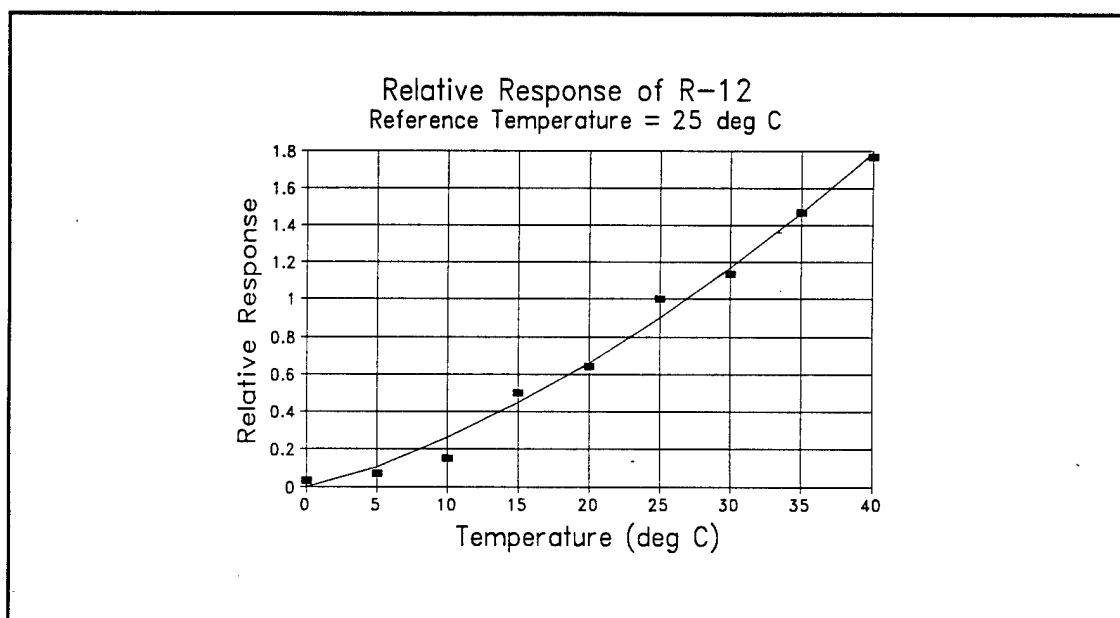
Figure 4.5 - Relative Response of R-12 Versus Temperature

61
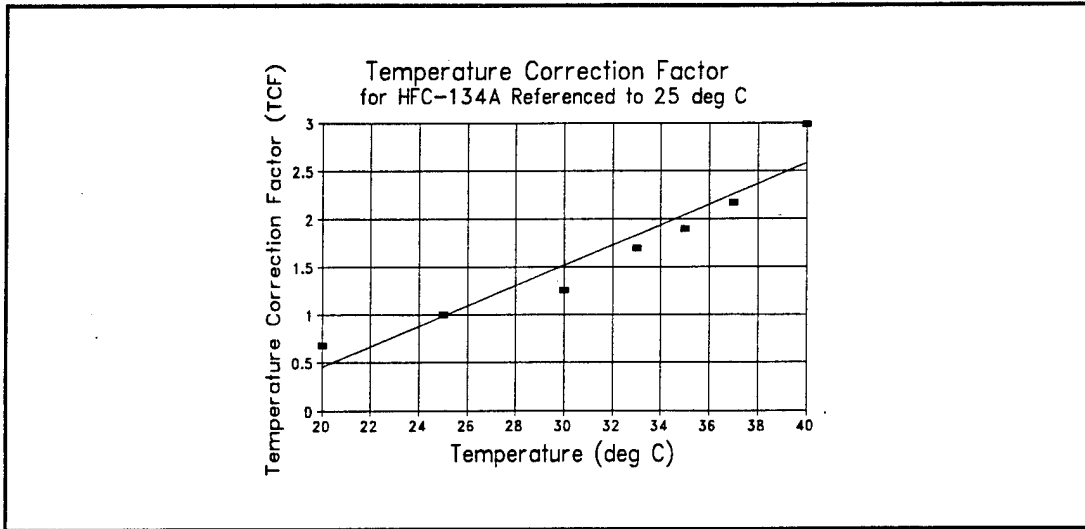
Figure 4.6 - Temperature Correction Factor for HFC
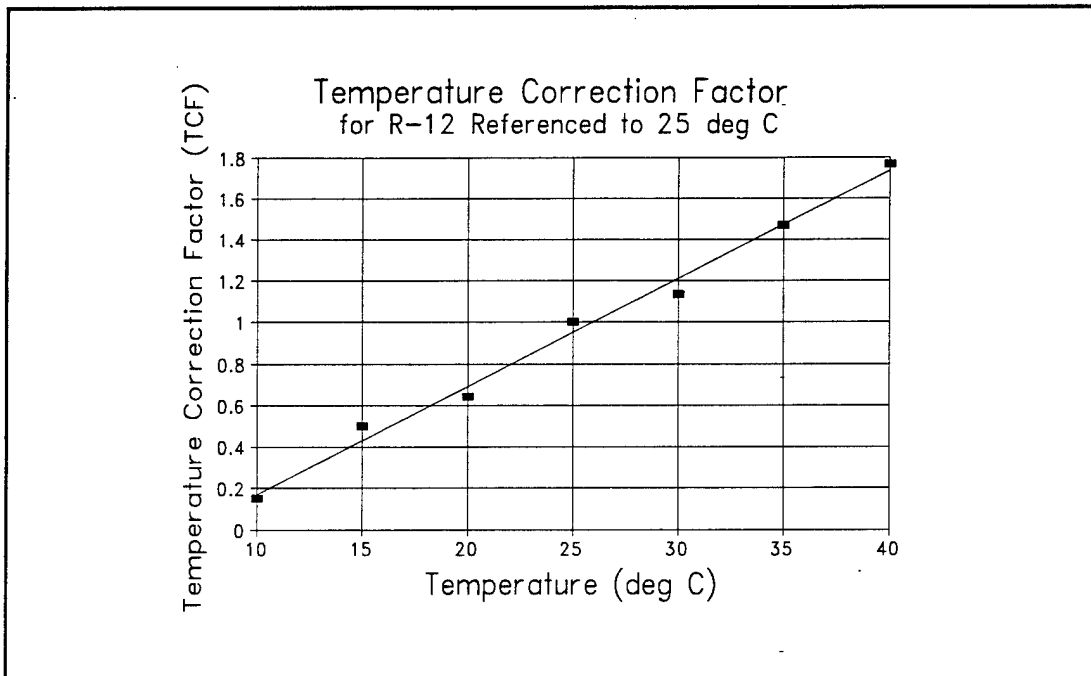
Figure 4.7 - Temperature Correction Factor for R-12
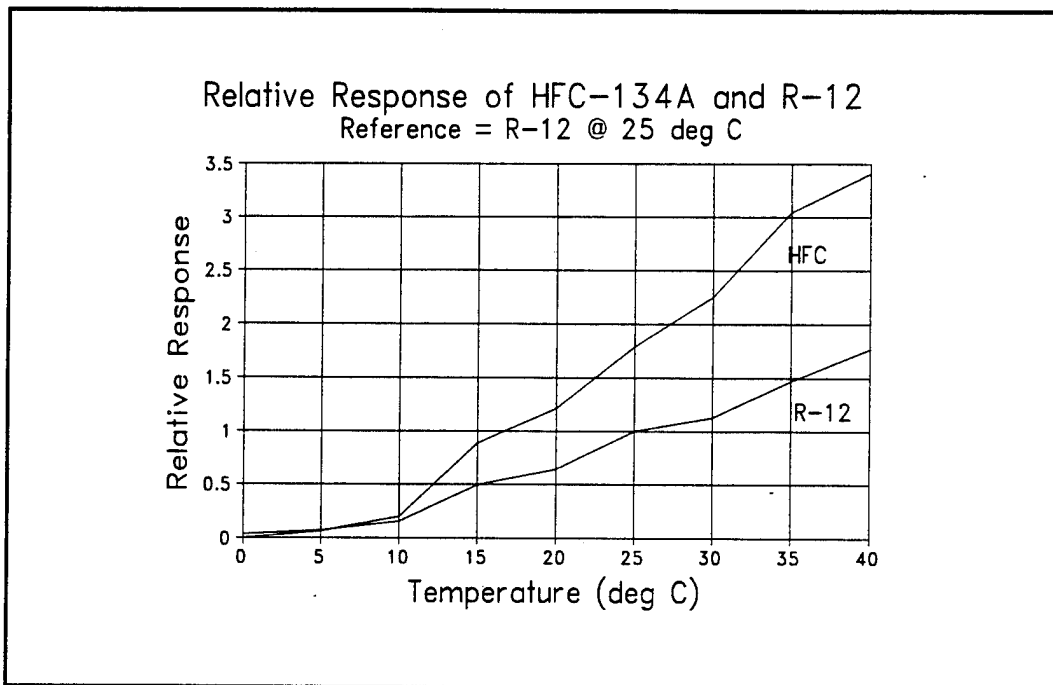
Figure 4.8 - Comparison of Temperature Responses of HFC and R-12

Since both dosimeters were irradiated between 0 and 40 degrees Celsius, a comparison was made between the responses of the dosimeters in this range. Figure 4.8 shows the response of the HFC and R-12 normalized to the response of the R-12 at 25 degrees Celsius. From this graph it can be seen that although the HFC dosimeter did not give a flat response as predicted, it is approximately 2 times as sensitive as the R-12 dosimeter from approximately 15 to 40 degrees Celsius.

4.4 Theoretical Analysis

The experimental results show that the response of the HFC dosimeter is not flat

as predicted by Rich, but rather its response increases with increasing temperature. Because of this unexpected result, further analysis was conducted into the theoretical response of the HFC compound.

Figure 4.9 shows the critical energy required to form a bubble (E_c) and the critical radius of the bubble determined by Rich.[1] From this graph it can be seen that as temperature increases, E_c decreases and becomes very low at temperatures above 20 degrees Celsius. From this graph it can be concluded that at temperatures above 20 degrees a recoil ion produced from any of the constituents of HFC (carbon, fluorine, and hydrogen) will most likely exceed E_c.
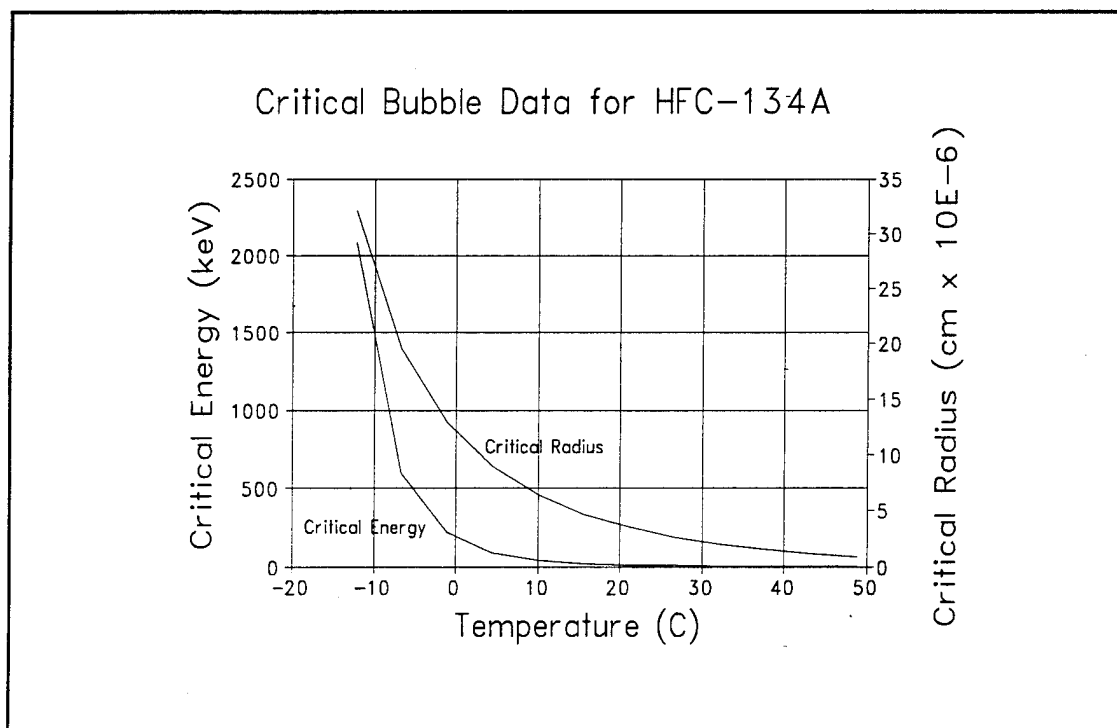
Figure 4.9 - Critical Energy and Critical Radius Versus Temperature for HFC

Rich's conclusion that HFC will have a flat temperature response was based on his graph of the HFC predicted response, Figure 4.10.[1] Rich reached the conclusion that at much higher temperatures (> 50 degrees Celsius), the effect of the hydrogen atoms will eventually cause the overall response of the compound to increase. It is important to note that this graph is based solely on a 2.1 MeV neutron.
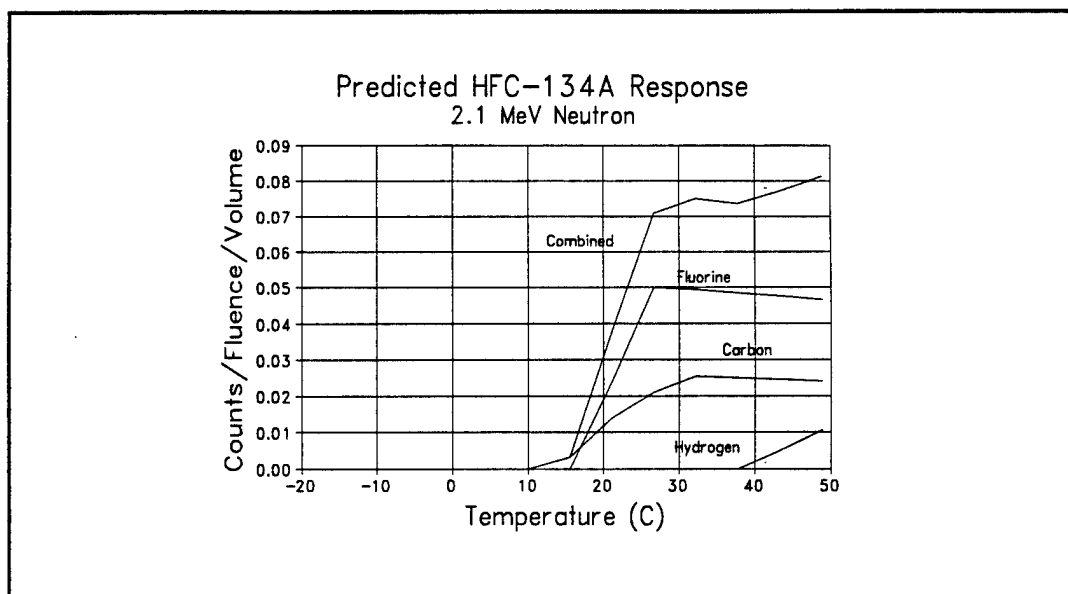
Figure 4.10 - Predicted HFC Response Versus Temperature

Figure 4.11 is a graph developed by Rich showing the stopping power (dE/dX) of the components of the HFC compound.[1] From this graph Rich assumed the stopping power of the hydrogen to be negligible compared to carbon and fluorine. This assumption is valid for neutron energies above 1 MeV, but not for neutron energies less than 1 MeV where the stopping power of hydrogen becomes significant.
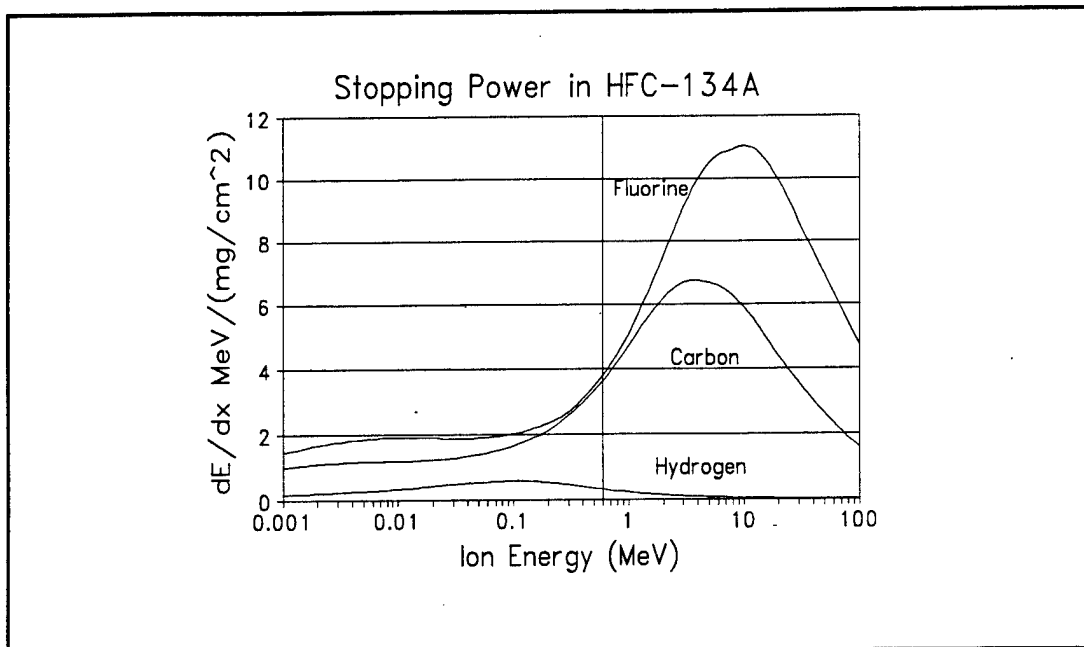
Figure 4.11 - Stopping Power in HFC

Figure 4.12 is a graph of the neutron energy spectrum emitted from a bare Cf^{252} source, the source used for the temperature response studies.[1] From this graph it can be seen that Cf^{252} emits neutrons from < 1 to > 10 MeV, and although the average neutron energy is greater than 1 MeV, there is a significant number of neutrons with less than 1 MeV.

Based on these observations it can be concluded that the predicted response for HFC from a polyenergetic neutron source, like Cf^{252}, will not be flat as predicted, but will increase due to the recoil ions from hydrogen at higher temperatures. The effect of hydrogen is significant because of the lower energy neutrons emitted from a polyenergetic source.
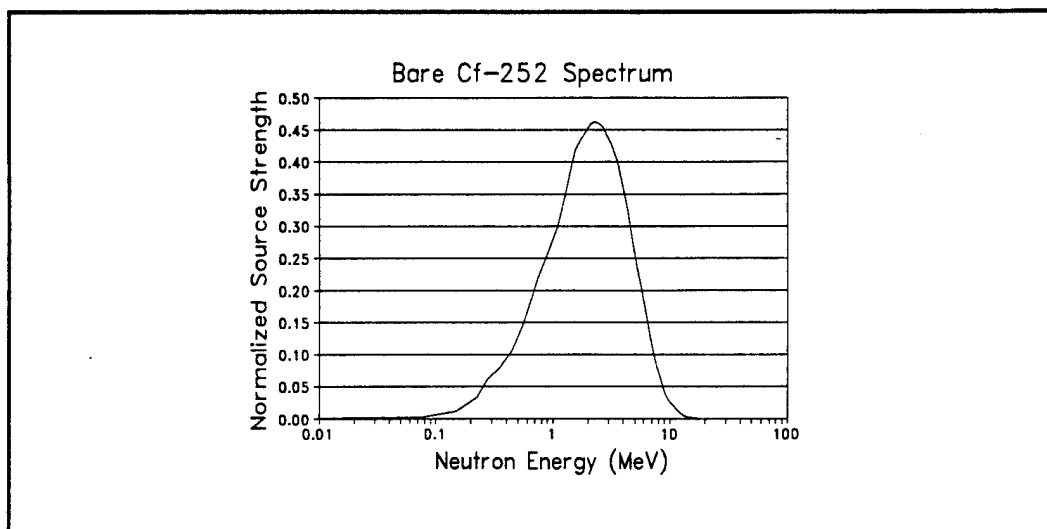
Figure 4.12 - Bare Cf^{252} Spectrum

4.5 Conclusions

Based on the experiments with the Cf^{252} source at USNA, it can be concluded that the response of the HFC and R-12 dosimeters increases with increasing temperature from 0 to 50 degrees Celsius for HFC and 0 to 40 degrees Celsius for R-12. Additionally it can be seen that there is a region for each dosimeter where the response for each dosimeter is nearly linear with temperature. This region is 20 to 40 degrees Celsius for HFC and 10 to 40 degrees Celsius for R-12. The TCF's allow the response of the dosimeters to be temperature corrected in the linear regions of the particular dosimeter. It is also important to note that although the HFC did not give the desired flat response, it did give approximately twice the response of the standard, commercially available R-12 dosimeter from 10 to 40 degrees Celsius.

Chapter V

Neutron Energy Studies

The objective of the neutron energy studies is given. The three megavolt (MV) tandem accelerator used is described. The neutron energy source, the $Li^7(p,n)Be^7$ reaction, is discussed. The experimental setup, results, and conclusions are outlined.

5.1 Introduction

Because of the possible variability in the amount of moderating material around nuclear munitions, it is desired that any arms control verification device based on emitted neutron radiation give a constant response over a range of neutron energies. This would prevent the verification device from giving erroneous readings due to neutron attenuation around the source, and would allow the device to give a response dependent on the total number of neutrons emitted.

As previously mentioned, the studies by Rich and Harper concluded that there was a critical energy (E_c) that must be deposited in the bubble material to cause bubble nucleation.[1,10] This E_c translates into a minimum incident neutron energy to cause bubble nucleation. Apfel has determined through his own research that the minimum neutron energy required to cause pops in the R-12 SDD and the HFC SDD is 100 keV.[20] This is the reason that he labels these dosimeters the SDD-100 and the SDD-100S respectively, with the 100 corresponding to a 100 keV threshold energy. What is not mentioned by Apfel is the response of the bubble dosimeters as incident neutron energy increases above the threshold.

The objective of this research is to determine the response of the Apfel R-12 and HFC bubble dosimeters as a function of neutron energy. To accomplish this, tests were conducted at NSWC using a three MV tandem proton accelerator in conjunction with a Li^7 target to produce neutrons at varying energies to irradiate both dosimeters.

5.2 Three MV Tandem Proton Accelerator

Figure 5.1 is a block diagram of the proton accelerator used at NSWC.[21] In this accelerator, positive hydrogen ions (protons) from the RF source are passed through rubidium vapor to add electrons and create negative hydrogen ions. This negative ion beam passes through the injector magnet (IM) into the low energy side of the three MV tandem accelerator (ACC) which causes the ion beam to accelerate to the center of the ACC where electron stripping is performed with nitrogen gas to create a positive ion beam (a proton with no electrons). This positive beam is then accelerated through the second half of the ACC. Because the charge of the ion beam is reversed in the middle of the ACC, the beam is accelerated twice, hence the name tandem accelerator. By controlling the terminal voltage (V_t) on the ACC, the energy of the proton beam exiting the ACC (E_p) can be controlled and is equal to $2*V_t$. After exiting the ACC, the proton beam passes through a 90 degree analyzing magnet (AM) which separates any foreign ions. The pure proton beam is then sent through the switching magnet (SM) into one of 5 experimental beam lines. In this experiment the proton beam was sent into the central beam line for neutrons (N) where a Li^7 target was placed.

Block Diagram of 3 MV Tandem Accelerator
at NSWC

RF — ion source for gas
SN — ion source for solid
IM — injector magnet
ACC — 3 MV accelerator
AM — analyzing magnet
SM — switching magnet
N — central beam for neutrons
Li — lithium target
BD — Apfel bubble dosimeters

Figure not to scale
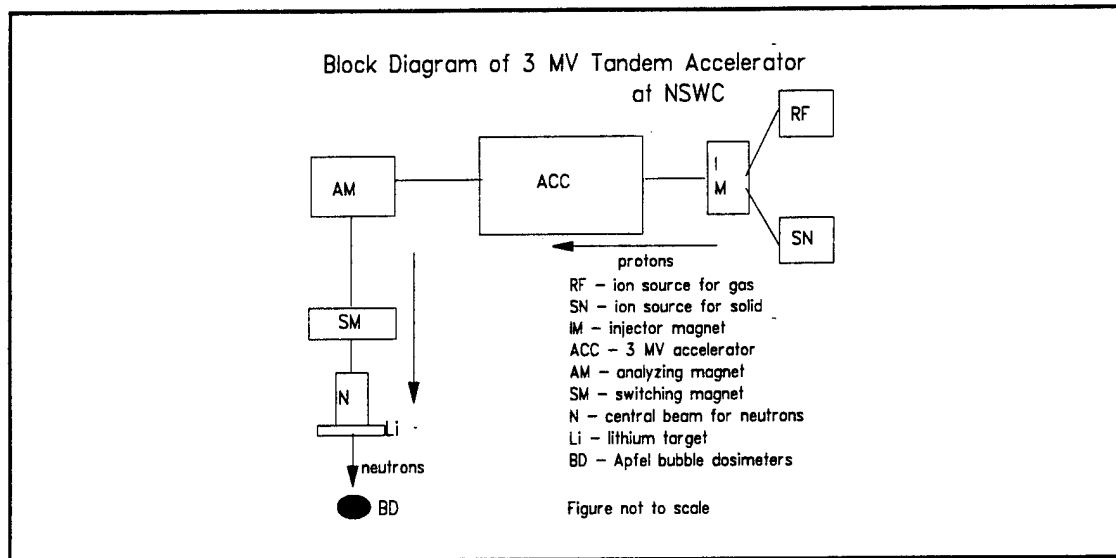
Figure 5.1 - Neutron Energy Studies Setup

5.3 $Li^7(p,n)Be^7$ Reaction

The neutron source for this experiment is the $Li^7(p,n)Be^7$ reaction that occurs as

the proton beam strikes the lithium target. This reaction is used since the energy of the

neutron (E_n) can be accurately determined knowing E_p and the emission angle in the

laboratory system (θ). Through analysis of this reaction, it can be determined that there

is a minimum proton energy (E_{th}) of 1.88 MeV required for the reaction to occur.[22] Figure

5.2 shows E_n as function of E_p for $\theta = 0$ degrees.[22] Also of importance is the cross section

(σ) for the reaction which is dependent on E_p. Figure 5.3 shows σ as a function of E_p.[22]

Although σ does not change E_n, it does change the number of neutrons produced from a

given number of protons.
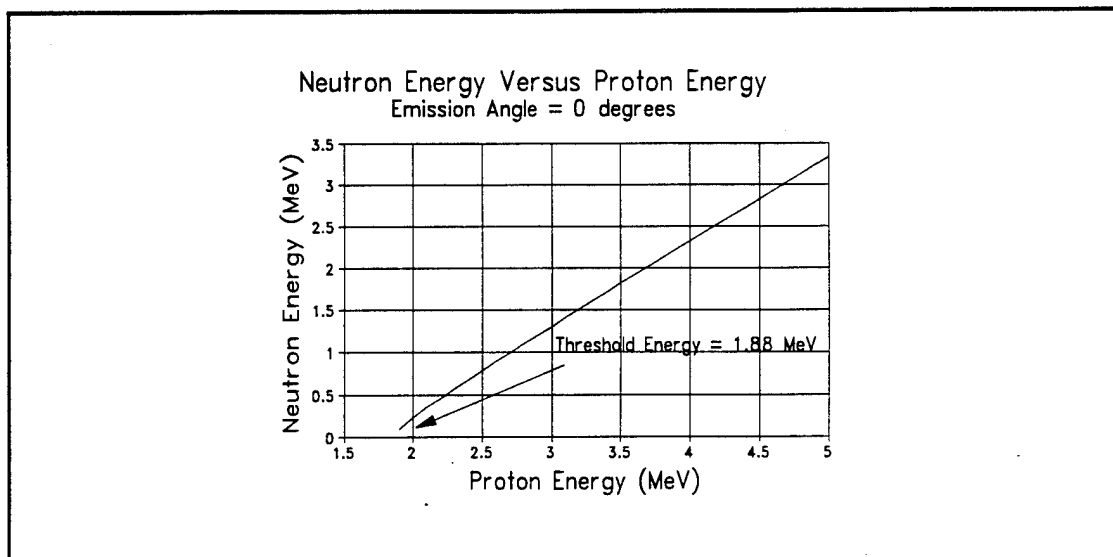
Figure 5.2 - Neutron Energy Versus Proton Energy
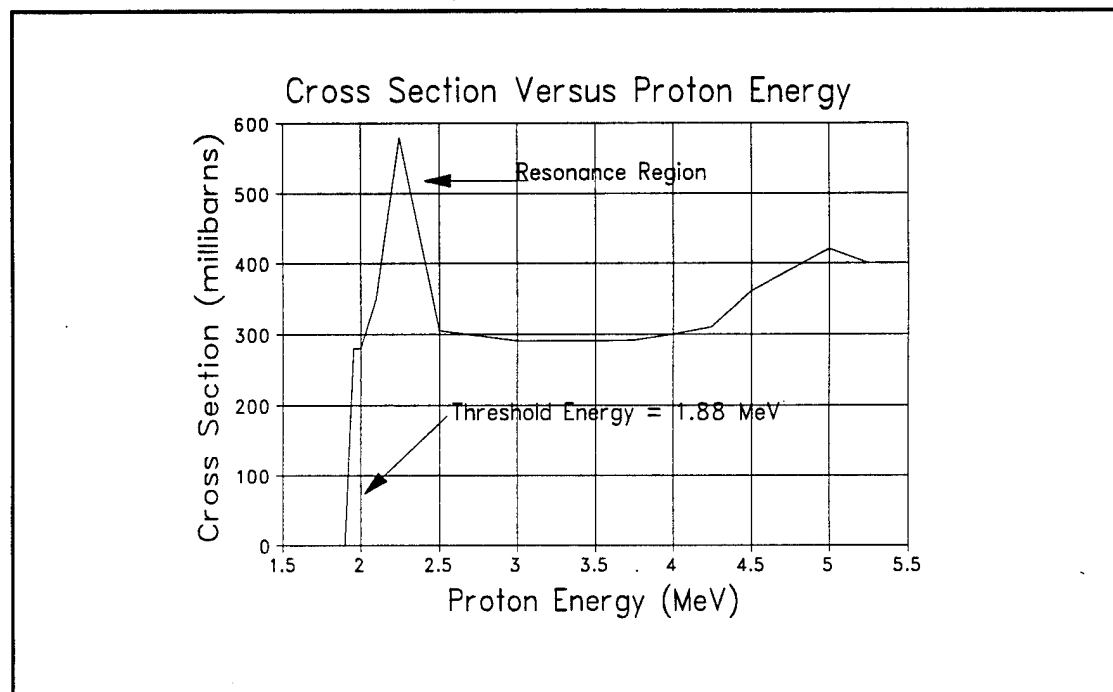
Figure 5.3 - Li^7(p,n)Be^7 Cross Section Versus Proton Energy

71

5.4 Experimental Setup

For this experiment, 2 ASM's, one containing an R-12 SDD and the other an HFC SDD, were placed in a covered beaker approximately 8 inches behind the Li^7 target. The temperature inside the beaker was controlled and recorded with an electronic heater connected to a thermocouple. E_p was controlled by changing V_t on the ACC as mentioned earlier, and θ was equal to zero for all irradiations. Thus, using Figure 5.2, E_n could be determined and controlled for all irradiations.

The number of protons hitting the target was controlled by measuring the total charge delivered through the accelerator. Irradiation time and charge rate (beam current) were determined in order to give a desired charge. In addition to the bubble dosimeters, an AN-PDR 70 neutron rem-meter was irradiated at the same distance to measure the dose rate for the experiment. This dose rate was kept to <200 mrem per hour for each irradiation due to Apfel's recommendation that the dosimeter not be used in fields >300 mrem per hour.[20]

5.5 Experimental Results

Both dosimeters were irradiated three times at neutron energies of 0.085, 0.2, 0.55, 0.9, 1.3, 1.7, 2.1, and 2.5 MeV wherein a new dosimeter was used for each energy level. For each irradiation, a set amount of charge (number of protons) was delivered to the dosimeters. The 1.7 MeV point was the first test conducted, and the dosimeters were irradiated with 40 μC total charge. From this test it was concluded that 20 μC would be sufficient for the remaining tests except for 0.085 and 0.2 MeV where a higher charge

(223 μC and 100 μC respectively) was needed to give sufficient response.

The charge delivered in each test was multiplied by the cross section corresponding to the E_p for that test, found from Figure 5.3, to give a value proportional to the fluence of neutrons delivered to the dosimeters. The response of each individual irradiation was temperature corrected using the TCF's generated in Chapter IV. Because the highest total number of droplets ever depleted was only 1684 (for HFC at 1.7 MeV), corresponding to a sensitivity correction of 1.075, no sensitivity degradation factor was included.

The responses from the three irradiations for each dosimeter at each neutron energy level were then averaged to give an average number of temperature corrected pops at each energy level. This value was then divided by the fluence for that energy level to give a value corresponding to the response per neutron fluence at each neutron energy level. All calculated values for both dosimeters are found in Appendix H.
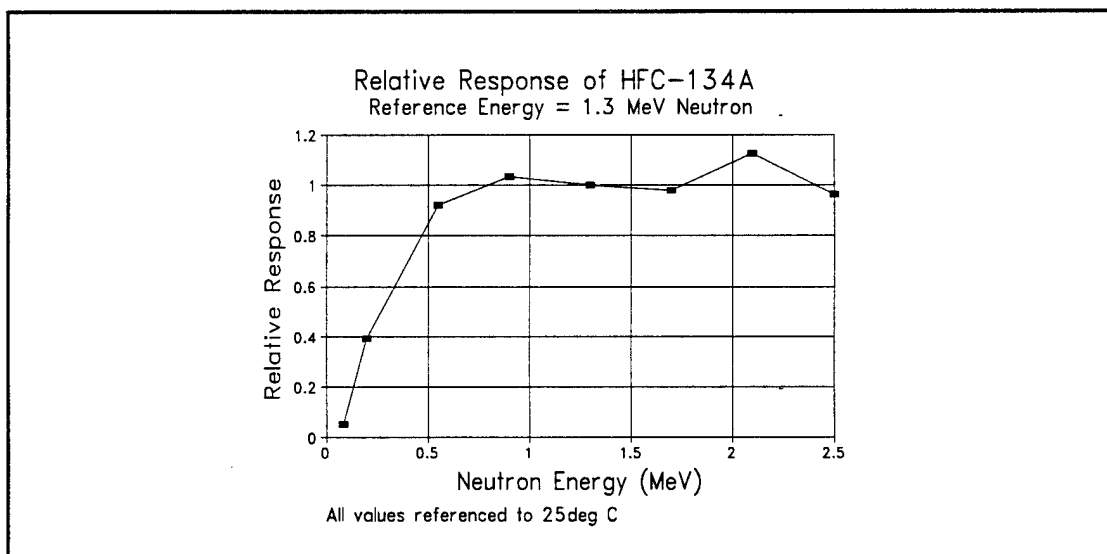
Figure 5.4 - Relative HFC Response Versus Neutron Energy

The response per fluence for each dosimeter was then normalized to the response per fluence at 1.3 MeV for each dosimeter. Figures 5.4 and 5.5 show the normalized response for HFC and R-12 respectively.
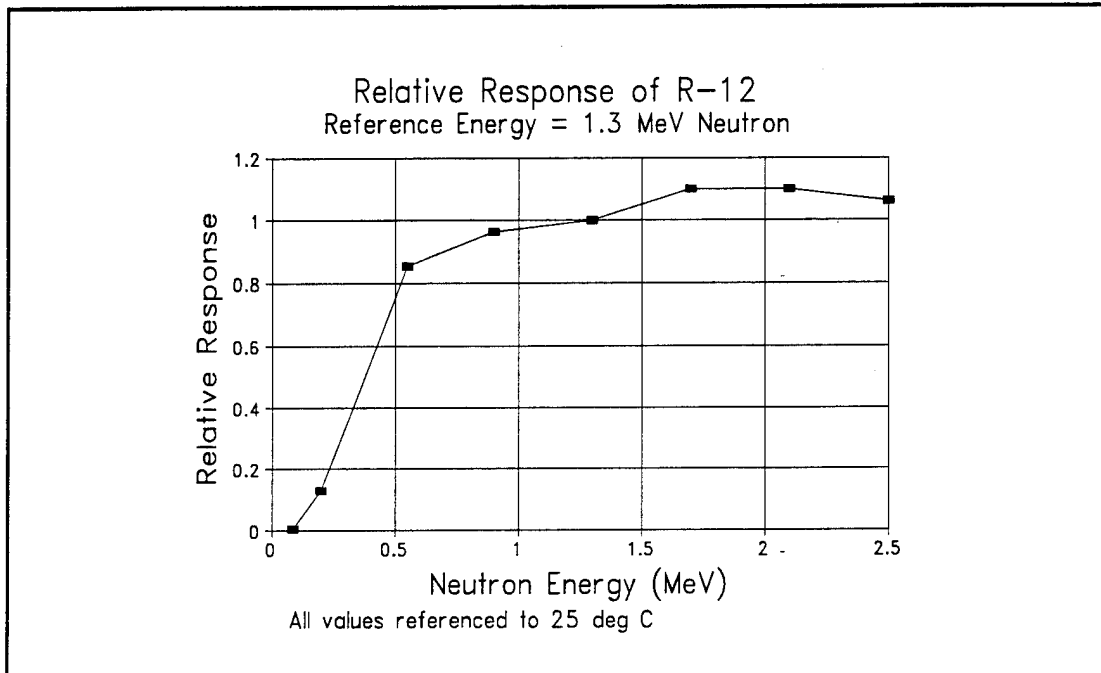
Figure 5.5 - Relative R-12 Response Versus Neutron Energy

5.6 Conclusions

Figures 5.4 and 5.5 show that the response for each dosimeter is relatively constant above 0.9 MeV for R-12 and 0.5 MeV for HFC. These figures also show that the response at 0.085 MeV for both dosimeters is nearly zero which is close to the threshold of 100 keV given by Apfel. This conclusion is very favorable since it indicates that the bubble dosimeters would give a constant response and predictable response to fission energy neutrons (approximately 1 to 2.5 MeV.)

Chapter VI

Conclusions and Recommendations

The initial tasks assigned by DNA for this research are delineated. The methods used to perform these tasks and conclusions drawn from them are outlined. Recommendations are made regarding the use of bubble dosimeters for treaty verification applications.

6.1 Conclusions

This research was performed under the auspices of DNA in order to determine the feasibility and practical procedures required to use bubble dosimeters for treaty verification applications. The tasks necessary to accomplish this as determined by DNA are listed in Table 6.1.[23]

Task 1 was conducted during the summer of 1993 through contact with the bubble dosimeter vendors, BTI and Apfel. For economic reasons it was decided that Apfel would be selected to investigate the feasibility of incorporating the alternate materials found by Rich. These alternate materials included HFC-134A (HFC), propane, and propylene. Research by Apfel concluded that of these materials only HFC-134A was stable in the Apfel SDD. Based on his own conclusions, Apfel recommended the use of hexafluorpropylene (HFP) as an alternate material. For these reasons HFC and HFP were chosen to be implemented in the Apfel dosimeters for their theoretical temperature response characteristics.

Table 6.1 - Project Tasks as determined by DNA

Task #	Task
1	Determine the feasibility of manufacturing bubble dosimeters incorporating alternate materials found in Rich's studies
2	Acquire sufficient number of dosimeters with these alternate materials
3	Identify bubble dosimeters with the highest sensitivity possible in order to maximize their counting efficiency to neutron emissions typical of nuclear weapon warheads
4	Perform comparative testing of bubble dosimeters with alternate materials
5	Investigate the reusability of the bubble dosimeters
6	Develop operational procedures for making field measurements to determine the presence or absence of nuclear warheads
7	Evaluate the procedures under Task 6 using a laboratory mockup of a nuclear warhead
8	Provide a final report including a description of all tests, all raw data, methodologies used to analyze data, conclusions, and recommendations regarding the suitability of bubble dosimeters for field use in arms control warhead inspection applications

Task 2 was accomplished in the fall of 1993 with the acquisition of 50 SDD-100S dosimeters containing HFC as the droplet material and 50 SDD-10 dosimeters containing HFP as the droplet material. These dosimeters were designed with Apfel's original design considerations, i.e. a reusable 4 ml vial containing 24,000 droplets.

Task 3 was accomplished by communication with the bubble dosimeter vendors before manufacture. In both dosimeters the sensitivity is limited by the number of droplets that can be contained in the dosimeter. Although the BTI dosimeters did not incorporate

the alternate materials, they were used in this research and were manufactured with the highest sensitivity possible. Normal BTI dosimeters have sensitivities of approximately 10 bubbles per mrem while the dosimeters used in this research had sensitivities ranging from 30 to 50 bubbles per mrem.

During the course of this research, Apfel has researched the possibility of enlarging his dosimeters to contain 40 ml of droplet material. These dosimeters were not available at the time of this research but, if manufactured, should show a greatly increased sensitivity.

Task 4 was accomplished through the 4 objectives as set forth in the introduction to this report. The comparative testing of the dosimeters was to include the following areas: (1) flatness of response versus temperature, (2) linearity of response as a function of neutron energy, (3) predictability and repeatability of measurements, (4) bubble growth rate, (5) dynamic range, and (6) insensitivity to gamma radiation. Through the research reported in Chapter IV, it was concluded that the response of the HFC and R-12 Apfel dosimeters was not constant with temperature, although it was concluded that the response of each dosimeter was approximately linear in a useful temperature band. Because the alternate materials were not implemented in the BTI dosimeters, no determination of their temperature response was made.

Through the research reported in Chapter V, it was concluded that the response of the HFC and R-12 dosimeters is essentially constant from approximately 0.9 MeV to 2.5 MeV, which roughly corresponds to the fission neutron energy spectrum. From the research described in Chapter IV and V, where the same source was used, it can also be

concluded that the response of the dosimeters is linear with respect to irradiation time.

During the experiments of Chapter IV and V, each test was conducted three times. The results from these were then averaged and a standard deviation was calculated. From analysis of these results it can be concluded that the response of the HFC and R-12 dosimeters is predictable, and the repetition of these tests shows that the measurements are repeatable. Similar conclusions can be drawn regarding the BTI dosimeter based on the repeated procedures discussed in Chapter II.

As mentioned in Chapter I, the bubbles formed in the Apfel dosimeter rise out of the gel material after formation. Because of this, there is no significance of bubble growth after irradiation, and therefore, no bubble growth analysis was conducted.

The dynamic range of the BTI dosimeter is determined by the maximum number of bubbles that can be effectively counted using the optical reader. From the conclusions in Rich's report, the highest number of bubbles that can be counted effectively is approximately 600.[1] From the data taken and presented in this report, it was seen that as the number of bubbles increased, the standard deviation of the averages increased, thus increasing the uncertainty associated with the readings. For this reason all experiments with the BTI were planned so that the number of bubbles produced would be less than 400.

Because neutron interactions within the Apfel dosimeters result in droplet depletion, the dynamic range of the Apfel dosimeters is limited by the number of droplets contained initially within the dosimeter. Also because of this droplet depletion, the sensitivity of the Apfel dosimeters decreases with use. To account for this, a sensitivity correction factor (SCF) was applied as described in Chapters IV and V. The irradiations

with the Apfel dosimeters were conducted so that no more than 6,000 droplets would be depleted. This was done to prevent excessive SCFs.

The gamma sensitivities of the BTI and Apfel R-12, HFC, and HFP dosimeter were researched as reported in Chapter III. From the results of these tests, it was concluded that the BTI and Apfel R-12 and HFC dosimeters were insensitive to gamma radiation up to 5,000 rads, and the Apfel HFP dosimeter was gamma sensitive at 50 rads gamma dose. It was also concluded that the ASM should not be used at high gamma dose levels.

In the test described in Chapter II, many of the BTI bubble dosimeters were reused. The variations in the responses for these tests were small and can be attributed to experiment related statistics rather than any degradation of performance of the dosimeters. Similarly during the research presented in Chapter III, it was noted that the gamma insensitivity of the BTI dosimeters did not change with reuse. For tests involving the Apfel dosimeters, it was concluded that the response of the Apfel dosimeter does decrease with reuse, but this degradation could be compensated.

Tasks 6 and 7 were accomplished during a summer internship with LANL through the SARA program. Because of damage to the Apfel dosimeters during shipment, only the response of the BTI dosimeters was studied at LANL. The results from Chapter II show that the BTI dosimeters are capable of measuring the emitted neutrons from a laboratory mockup of a warhead. In order to accomplish this it was necessary to place the dosimeters on contact with the source and allow them to irradiate for several hours.

Bubble dosimeters have several characteristics that allow them to be a possible candidate for treaty verification applications. Their small size, lack of electronics, and non-obtrusive data collection capability allow them to be easily used in the field. They also show a constant response with neutron energies from 0.9 to 2.5 MeV, and although their response is not constant with temperature, it can be corrected in a useful temperature band. It has also been shown that they are responsive to the neutron energy and intensity associated with nuclear warheads.

The major drawback to the use of bubble dosimeters for treaty verification applications is their low sensitivity. The procedures necessary to evaluate a suspected warhead source require a long period of time as well as close proximity to the source. The bubble dosimeter did not meet DNA's operations criterion of a few minutes counting time for this application.

6.2 Recommendations

It was shown in this research that several dosimeters could be irradiated around a single suspected warhead source. Due to the low sensitivities of the bubble dosimeters, this procedure would be necessary in order to achieve a high enough response to distinguish a nuclear from non-nuclear source. This procedure was detailed in Chapter II in the discussion of the device response uncertainty. The other alternative to this procedure is to develop bubble dosimeters with greatly increased sensitivities. This research is currently being done for the Apfel dosimeters. Construction and evaluation of new bubble dosimeters with increased sensitivities would greatly enhance the potential use of bubble dosimeters for treaty verification applications.

References

1.   J. C. Rich, M. J. Harper, and M. E. Nelson, "Bubble Dosimeter Suitability For Nuclear Arms Control," Report presented to Defense Nuclear Agency, July 1993.

2. J. McNeilly and B. Rothstein, "Radiation Detection Equipment (RDE) Comparative Evaluation Test Program," Report presented to Defense Nuclear Agency, July, 1993.

3.   P. E. Fehlau, "Portable Radiation-Detection Instruments for Distinguishing Nuclear from Non-nuclear Munitions," *Conference Record of the 1991 IEEE Nuclear Science Symposium*, Santa Fe, NM, 1991.

4.   P. E. Fehlau, "Field-Trial Results for Pre-Flight Non-Nuclear Verification in Air Force NELA Flight Tests," *Los Alamos National Laboratory document LA-12006-MS*, Los Alamos, NM, 1991.

5.   R. E. Apfel, U.S. Patent No. 4,143,274 (6 March 1979).

6.   H. Ing and H. C. Birnboim, U.S. Patent No. 4,613,758 (23 September 1986).

7. R. E. Apfel, "The Superheated Drop Detector," *Nucl. Instr. and Meth.*, 1979.

8. R. E. Apfel, U.S. Patent No. 4,350,607 (21 September 1982).

9. R. E. Apfel, Y-C Lo, and S. C. Roy, "Superheated Drop Detector: A Potential Tool in Neutron Research," *Nucl. Instr. and Meth.*, 1987.

10. M. J. Harper, "A Theoretical Model of a Superheated Liquid Droplet Neutron Detector," Ph.D. Dissertation, University of Maryland, Department of Chemical and Nuclear Engineering (1991).

11. M. A. Buckner, "Improving Neutron Dosimetry Using Bubble Detector Technology," *Oak Ridge National Laboratory document ORNL/TM-11916*, Oak Ridge, TN, 1993.

12. D. R. Sisk, K. L. Smith, and R. E. Apfel, "Neutron Detection Based on Superheated Materials," *IEEE Transactions on Nuclear Science*, vol. 37, no. 2, April 1990.

13.   M. Millett, F. Munno, D. Ebert, and M. E. Nelson, "An Evaluation of the BD-100R Rechargeable Neutron Bubble Dosimeter," *Health Physics*, vol. 60, no. 3, March 1991.

14. Bubble Technology Industries, Inc., <u>BTI Bubble Reader BDR-Series II User's Manual, Rev 3</u>, July 3, 1991.

15. Personal communication with Mr. George Neuman, Los Alamos National Laboratory, June 1993 through July 1993.

16. E. J. Reilly, "Evaluation of Bubble Dosimeter Response to Neutron Radiation," *Trident Scholar Report No. 159*, United States Naval Academy, Annapolis, Md, 1989.

17. M. J. Wilson, "Evaluation of Neutron Dose Measurement Techniques for Use in a Shipboard Environment," *Trident Scholar Report No. 174*, United States Naval Academy, Annapolis, MD, 1990.

18. G. F. Knoll, <u>Radiation Detection and Measurement</u>, John Wiley and Sons, New York, NY, 1989.

19. Personal communication with Bubble Technologies, Inc., May 1993 to May 1994.

20. Personal communication with Apfel Enterprises, May 1993 to May 1994.

21. J. L. Price, D. J. Land, S. H. Stern, N. A. Guardala, P. K. Cady, D. G. Simons, M. D. Brown, J. G. Brennan, and M. F. Stumborg, "An Overview of the Ion-Beam Analysis Laboratory at White Oak," *Nucl. Instr. and Meth.*, 1991.

22. J. B. Marion and J. L. Fowler, <u>Fast Neutron Physics Part I</u>, Interscience Publishers, Inc., New York, NY, 1960.

23. Personal communication with LTCOL Benard Simelton, Defense Nuclear Agency, May 1993 to May 1994.

Appendix A
Raw Bubble Reader Data for All Tests

Chapter 2 - Special Source Test

Test 2.1 - Background in ADL

Dosimeter Group	Reading: 1	2	3	4	Average	Standard Deviation
1	4	4	4	4	4	0
2	4	4	4	4	4	0
3	2	2	2	2	2	0

Test 2.2 - Background in Kiva 2

Dosimeter Group	Reading: 1	2	3	4	Average	Standard Deviation
1	64	60	63	61	62	1.83
2	78	79	79	82	79.5	1.73
3	43	38	40	40	40.25	2.06

Test 2.5 - AmLi

Dosimeter Group	Reading: 1	2	3	4	Average	Standard Deviation
A	211	208	228	217	216	8.83
	271	250	265	270	264	9.70
	190	186	189	169	183.5	9.81
B	201	192	192	192	194.25	4.50
	231	240	227	227	231.25	6.13
	220	230	219	237	226.5	8.58
C	144	137	157	143	145.25	8.42
	225	241	205	229	225	14.97
	239	221	222	214	224	10.61
D	105	98	108	101	103	4.40
	141	157	153	159	152.5	8.06
	120	115	130	125	122.5	6.45
E	155	160	151	158	156	3.92
	126	139	124	144	133.25	9.78
	149	158	153	152	153	3.74
F	151	148	155	143	149.25	5.06
	134	136	144	140	138.5	4.43
	149	153	141	139	145.5	6.61

Dosimeter Group	Reading: 1	2	3	4	Average	Standard Deviation
H	57	55	55	57	56	1.15
	68	68	72	72	70	2.31
	70	61	66	62	64.75	4.11
	42	50	49	47	47	3.56
	76	73	86	70	76.25	6.95
	66	63	57	66	63	4.24
	72	67	67	67	68.25	2.50
	67	71	66	64	67	2.94
	80	72	70	73	73.75	4.35

Test 2.6 and 2.7 - Special Source 1

Dosimeter Group	Reading: 1	2	3	4	Average	Standard Deviation
A1	107	103	112	107	107.25	3.69
	119	114	118	108	114.75	4.99
	111	99	105	101	104	5.29
A2	87	86	87	93	88.25	3.20
	81	90	84	83	84.5	3.87
	88	97	88	92	91.25	4.27
B	91	88	91	91	90.25	1.50
	56	62	58	58	58.5	2.52
	62	65	60	64	52.75	2.22
C	79	86	84	79	82	3.56
	129	136	135	129	132.25	3.77
	109	120	110	111	112.5	5.07
D	87	82	86	89	86	2.94
	109	99	97	92	99.25	7.14
	96	102	98	98	98.5	2.52
E	122	113	117	113	116.25	4.27
	90	96	93	92	92.75	2.50
	97	99	103	105	101	3.65
F	111	96	88	100	98.75	9.57
	105	107	111	109	108	2.58
	122	109	124	115	117.5	6.86

Tests 2.8 and 2.9 - Special Source 2

Tests 2.8 and 2.9 - Special Source 2

| Dosimeter | Reading: | | | | | Standard |
Group	1	2	3	4	Average	Deviation
A	77	80	76	77	77.5	1.73
	72	69	72	71	71	1.41
B	87	88	95	84	88.5	4.65
	82	77	81	82	80.5	2.38
C	182	197	198	187	191	7.79
	183	203	196	185	191.75	9.43
D	79	83	76	69	76.75	5.91
	67	69	68	61	66.25	3.59
E	34	37	35	38	36	1.83
F	34	33	31	35	33.25	1.71
G	13	13	13	13	13	0.00
H	13	13	13	13	13	0.00
I	112	113	122	114	115.25	4.57
	86	82	81	85	83.5	2.38
	86	87	82	86	85.25	2.22
J	115	101	105	101	105.5	6.61
	139	140	148	138	141.25	4.57
	105	97	100	91	98.25	5.85
K	83	84	79	93	84.75	5.91
	106	102	88	103	99.75	8.02
	87	98	93	87	91.25	5.32
L	79	76	81	80	79	2.16
	108	97	107	99	102.75	5.56
	69	65	66	60	65	3.74

Group 4

Dosimeter Group	Reading: 1	2	3	4	Average	Standard Deviation
1	102	104	106	105	104.25	1.48
2	76	80	83	85	81	3.39
3	90	92	93	91	91.5	1.12
4	83	80	78	76	79.25	2.59
1	113	109	114	114	112.5	2.06
2	77	76	79	81	78.25	1.92
3	88	95	99	98	95	4.30
4	77	81	86	84	82	3.39
1	203	187	192	190	193	6.04
2	140	154	148	152	148.5	5.36
3	172	187	174	168	175.25	7.12
4	167	162	174	150	163.25	8.76
1	195	192	209	197	198.25	6.46
2	147	168	155	153	155.75	7.66
3	172	176	180	179	176.75	3.11
4	171	177	174	160	170.5	6.42
1	252	238	264	254	252	9.27
2	215	222	219	210	216.5	4.50
3	230	236	225	223	228.5	5.02
4	267	240	257	221	246.25	17.48
1	246	225	265	249	246.25	14.24
2	208	214	216	206	211	4.12
3	223	239	231	237	232.5	6.22
4	254	231	268	219	243	19.14

Group 5

Dosimeter Group	Reading: 1	2	3	4	Average	Standard Deviation
1	107	102	104	95	102	4.42
2	79	70	74	79	75.5	3.77
3	139	149	140	150	144.5	5.02
4	79	76	78	76	77.25	1.30
1	186	182	177	188	183.25	4.21
2	165	155	151	148	154.75	6.42
3	236	241	231	225	233.25	5.93
4	140	152	142	141	143.75	4.82
1	254	240	249	251	248.5	5.22
2	227	216	220	217	220	4.30
3	290	273	280	267	277.5	8.56
4	205	204	188	189	196.5	8.02
1	253	243	245	246	246.75	3.77
2	233	209	231	229	225.5	9.63
3	300	288	298	291	294.25	4.92
4	199	206	195	195	198.75	4.49

Group 6

Dosimeter Group	Reading: 1	2	3	4	Average	Standard Deviation
1	57	165	156	162	160	3.67
2	240	202	219	232	223.25	14.38
3	249	255	258	244	251.5	5.41
4	176	196	174	182	182	8.60
1	95	103	95	97	97.5	3.28
2	105	113	118	110	111.5	4.72
3	198	208	189	215	202.5	9.86
4	133	144	145	153	143.75	7.12
1	73	80	74	69	74	3.94
2	88	87	90	90	88.75	1.30
3	85	89	81	82	84.25	3.11
4	88	98	94	98	94.5	4.09

Group 7

Dosimeter Group	Reading: 1	2	3	4	Average	Standard Deviation
1	64	153	153	165	158.75	5.76
2	246	233	245	252	244	6.89
3	176	181	192	179	182	6.04
4	249	241	242	238	242.5	4.03
1	86	91	100	104	95.25	7.12
2	129	127	126	132	128.5	2.29
3	89	92	96	92	92.25	2.49
4	126	125	122	131	126	3.24
1	90	86	88	84	87	2.24
2	106	110	108	110	108.5	1.66
3	95	87	94	90	91.5	3.20
4	104	113	111	109	109.25	3.34

Appendix B
Calculated Data for AmLi (Test 2.5)

Calculated Data for AmLi (Test 2.5)

Background Calculation for ADL - Test 2.1

Dos #	Time (hr)	Bubbles	Sens (b/mr)	Normal (bub)	Rate (bub/hr)
1	17.25	4	49	4.08	0.237
2	17.25	4	40	5.00	0.290
3	17.25	2	34	2.94	0.171

Avg Background Rate: 0.232 bub/hr

Dos Std Pos	Dist (m)	Time (hr)	Bubbles	Sens (b/mr)	Normal (bub)	(bub/hr)	Rate (bub/hr)	Net (bub/hr)	Mean Std Dev
A	0.25	2.00	216	46	235	117	117	131	20.6
	0.25	2.00	264	39	338	169	169		
	0.25	2.00	183.5	44	209	104	104		
B	0.25	2.00	194.25	41	237	118	118		
	0.25	2.00	231.25	42	275	138	137		
	0.25	2.00	226.5	39	290	145	145		
C	0.25	2.00	145.25	33	220	110	110		
	0.25	2.00	225	39	288	144	144		
	0.25	2.00	224	42	267	133	133		
D	0.50	4.00	103	35	147	36.8	36.6	40	3.5
	0.50	4.00	152.5	57	134	33.4	33.2		
	0.50	4.00	122.5	35	175	43.8	43.5		
E	0.50	4.00	156	47	166	41.5	41.3		
	0.50	4.00	133.25	43	155	38.7	38.5		
	0.50	4.00	153	45	170	42.5	42.3		
F	0.50	4.00	149.25	46	162	40.6	40.3		
	0.50	4.00	138.5	41	169	42.2	42.0		
	0.50	4.00	145.5	41	177	44.4	44.1		
G	1.00	5.00	56	37	76	15.1	14.9	17	2.9
	1.00	5.00	70	36	97	19.4	19.2		
	1.00	5.00	64.75	39	83	16.6	16.4		
H	1.00	5.00	47	34	69	13.8	13.6		
	1.00	5.00	76.25	47	81	16.2	16.0		
	1.00	5.00	63	43	73	14.7	14.4		
I	1.00	5.00	68.25	34	100	20.1	19.8		
	1.00	5.00	67	44	76	15.2	15.0		
	1.00	5.00	73.75	33	112	22.3	22.1		

91

Data for NNV-470:

Dist (cm)	Counts (cts)	Counts (cts/sec)	Relative Sensitivity
3	10297	515	N/A
25	578	28.9	795
50	208	10.4	929
100	79.8	3.99	854

Counting time for the NNV-470 is 20 seconds

Relative Sensitivity is to BD-100R at same distance

Appendix C
Calculated Data for Special Source 1 (Test 2.6 and 2.7)

Calculated Data for Special Source 1 (Tests 2.6 and 2.7)

Background Calculation for Kiva 2 - Test 2.2

Dos #	Time (hr)	Bubbles	Sens (b/mr)	Normal (bub)	Rate (bub/hr)
1	22.58	362	43	72.09	3.192
2	22.58	379.5	87	45.69	2.023
3	22.58	340.25	57	35.31	1.563

Avg Background Rate:2.260 bub/hr

Dos Pos	Dist (m)	Time (hr)	Bubbles	Sens (b/mr)	Normal (bub)	Rate (bub/hr)	Net (bub/hr)	Mean (bub/hr)	Std Dev
A1	0.46	5.67	107	38	141	24.9	22.6	19.2	3.95
	0.46	5.67	115	59	97.2	17.2	14.9		
	0.46	5.67	104	41	127	22.4	20.1		
A2	-0.46	5.67	88.3	39	113	20.0	17.7	15.6	3.31
	-0.46	5.67	84.5	53	79.7	14.1	11.8		
	-0.46	5.67	91.3	41	111	19.6	17.4		
B	+-0.68	5.67	90.3	39	116	20.4	18.2	13.6	3.97
	+-0.68	5.67	58.5	37	79.1	14.0	11.7		
	+-0.68	5.67	62.8	42	74.7	13.2	10.9		
C	1.29	17.8	82.0	37	111	6.21	3.95	4.59	0.58
	1.29	17.8	132	53	125	7.00	4.74		
	1.29	17.8	113	43	131	7.34	5.08		
D	-1.29	17.8	86.0	35	123	6.89	4.63	4.08	1.12
	-1.29	17.8	99.3	55	90.2	5.06	2.80		
	-1.29	17.8	98.5	39	126	7.08	4.82		
E	1.46	17.8	116	54	108	6.04	3.78	4.42	0.86
	1.46	17.8	92.8	41	113	6.34	4.08		
	1.46	17.8	101	37	136	7.65	5.39		
F	-1.46	17.8	98.8	40	123	6.92	4.66	4.78	1.32
	-1.46	17.8	108	36	150	8.41	6.15		
	-1.46	17.8	118	57	103	5.78	3.52		

Appendix D
Calculated Data for Special Source 2 (Test 2.8 and 2.9)

Calculated Data for Special Source 2 (Test 2.8 and 2.9)

Dos Pos	Dist (m)	Time (hr)	Bubbles	Sens (b/mr)	Normal (bub)	Rate (bub/hr)	Net (bub/hr)	Mean (bub/hr)	Std Dev
A	-0.3	3.83	77.5	40	96.9	25.3	23.0	25.3	3.72
	-0.3	3.83	71	37	95.9	25.0	22.8		
B	0.3	3.83	88.5	35	126	33.0	30.7		
	0.3	3.83	80.5	39	103	26.9	24.7		
C	0.5	20.42	191	47	203	9.95	7.69	8.74	1.48
	0.5	20.42	191.75	39	246	12.0	9.78		
D	-0.5	20.42	276.75	46	83.4	4.09	1.83	1.71	0.16
	-0.5	20.42	66.25	42	78.9	3.86	1.60		
E	0.5831	3.83	36	55	32.7	8.54	6.28	6.10	0.25
F	0.5831	3.83	33.25	53	31.4	8.18	5.92		
G	-0.5831	3.83	13	59	11.0	2.88	0.62	1.47	1.21
H	-0.583	3.83	13	37	17.6	4.58	2.32		
I	0.8544	20.42	115.25	52	111	5.43	3.17	3.30	0.83
	0.8544	20.42	83.5	38	110	5.38	3.12		
	0.8544	20.42	85.25	47	90.7	4.44	2.18		
J	0.8544	20.42	105.5	38	139	6.80	4.54		
	0.8544	20.42	141.25	56	126	6.18	3.92		
	0.8544	20.42	98.25	47	105	5.12	2.86		
K	-0.854	20.42	84.75	48	88.3	4.32	2.06	2.52	0.96
	-0.854	20.42	99.75	53	94.1	4.61	2.35		
	-0.854	20.42	91.25	35	130	6.38	4.13		
L	-0.854	20.42	79	37	107	5.23	2.97		
	-0.854	20.42	102.75	55	93.4	4.58	2.32		
	-0.854	20.42	65	45	72.2	3.54	1.28		

Appendix E
Uncertainty Information for Special Source 1 and 2

Uncertainty Information for Special Source 1

Maximum Avg Count Rate-   17.4 bub/hr above background

Time with X Dosimeters:

Uncertainty (%)	Bubbles	1 (hr)	5 (hr)	10 (hr)	20 (hr)	50 (hr)
1.00	10000	574.7	114.9	57.47	28.74	11.49
1.25	6400	367.8	73.56	36.78	18.39	7.356
1.50	4444	255.4	51.09	25.54	12.77	5.109
1.75	3265	187.7	37.53	18.77	9.383	3.753
2.00	2500	143.7	28.74	14.37	7.184	2.874
2.25	1975	113.5	22.70	11.35	5.676	2.270
2.50	1600	91.95	18.39	9.195	4.598	1.839
2.75	1322	76.00	15.20	7.600	3.800	1.520
3.00	1111	63.86	12.77	6.386	3.193	1.277
3.50	816	46.92	9.383	4.692	2.346	0.938
4.00	625	35.92	7.184	3.592	1.796	0.718
4.50	494	28.38	5.676	2.838	1.419	0.568
5.00	400	22.99	4.598	2.299	1.149	0.460
5.50	331	19.00	3.800	1.900	0.950	0.380
6.00	278	15.96	3.193	1.596	0.798	0.319
6.50	237	13.60	2.721	1.360	0.680	0.272
7.00	204	11.73	2.346	1.173	0.586	0.235
7.50	178	10.217	2.043	1.022	0.511	0.204
8.00	156	8.980	1.796	0.898	0.449	0.180
8.50	138	7.955	1.591	0.795	0.398	0.159
9.00	123	7.095	1.419	0.710	0.355	0.142
9.50	111	6.368	1.274	0.637	0.318	0.127
10.00	100	5.747	1.149	0.575	0.287	0.115

Uncertainty information for Special Source 2

Maximum Avg Count Rate-　　　　25.3 bub/hr above background

		Time with X Dosimeters:				
Uncertainty		1	5	10	20	50
(%)	Bubbles	(hr)	(hr)	(hr)	(hr)	(hr)
1.00	10000	395.3	79.05	39.53	19.76	7.905
1.25	6400	253.0	50.59	25.30	12.65	5.059
1.50	4444	175.7	35.13	17.57	8.783	3.513
1.75	3265	129.1	25.81	12.91	6.453	2.581
2.00	2500	98.81	19.76	9.881	4.941	1.976
2.25	1975	78.08	15.62	7.808	3.904	1.562
2.50	1600	63.24	12.65	6.324	3.162	1.265
2.75	1322	52.27	10.453	5.227	2.613	1.045
3.00	1111	43.92	8.783	4.392	2.196	0.878
3.50	816	32.27	6.453	3.227	1.613	0.645
4.00	625	24.70	4.941	2.470	1.235	0.494
4.50	494	19.52	3.904	1.952	0.976	0.390
5.00	400	15.81	3.162	1.581	0.791	0.316
5.50	331	13.07	2.613	1.307	0.653	0.261
6.00	278	10.98	2.196	1.098	0.549	0.220
6.50	237	9.355	1.871	0.936	0.468	0.187
7.00	204	8.066	1.613	0.807	0.403	0.161
7.50	178	7.027	1.405	0.703	0.351	0.141
8.00	156	6.176	1.235	0.618	0.309	0.124
8.50	138	5.471	1.094	0.547	0.274	0.109
9.00	123	4.880	0.976	0.488	0.244	0.0976
9.50	111	4.380	0.876	0.438	0.219	0.0876
10.00	100	3.953	0.791	0.395	0.198	0.0791

Appendix F
Detailed Irradiation Histories of Each Bubble
Dosimeter Group in AFRRI Tests

Detailed Irradiation Histories of Each Bubble Dosimeter
Group in AFRRI Tests

Group 1:   Gam= 50 Rads

Gam ---->   Gam ----> Gam
(O)   (O)   (O)

Group 2:   Gam= 500 Rads

Am ---->   Gam ----> Gam
(O)   (O)   (O)

Group 3:   Gam= 5000 Rads

Gam ---->   Gam ----> Gam
(O)   (O)   (O)

Group 4:   Gam= 5000 Rads

Neut ---->   Gam ---->   Neut ---->   Gam ---->   Neut ---->   Gam
(89)   (92)   (170)   (175)   (236)   (233)

Group 5:   Gam= 5000 Rads

Neut ---->   Gam ---->   Neut ---->   Gam
(100)   (179)   (236)   (241)

Group 6:   Gam= 5000 Rads

Neut ---->   Rep ---->   Gam ---->   Neut ---->   Rep ---->   Gam
(204)   (O)   (O)   (139)   (O)   (O)

Neut ---->   Rep
(85)   (O)

Group 7:   Gam= 5000 Rads

Neut ---->   Rep ---->   Neut ---->   Rep ---->   Neut ---->   Rep
(171)   (O)   (111)   (O)   (99)   (O)

Gam
(O)

Notes: (1) Neut represents neutron irradiation
          (2) Gam represents gamma irradiation
          (3) Rep represents repressurization of dosimeter
          (4) Numvers represent number of bubbles present

Appendix G
Data for Temperature Tests

Data for Temperature Tests for HFC-1 34A

Temp (deg C)	Dinitial	Dfinal	Cfsens	Tasm (sec)	Cftime	Praw	Poor	Avg Pops	Std Dev
0	24000	24000	1.000	495	0.990	0	0	0	0
	24000	24000	1.000	485	1.010	0	0		
	24000	24000	1.000	487	1.006	0	0		
5	23991	23983	1.001	493	0.994	8	7.96	11.96	3.28
	23983	23967	1.001	491	0.998	16	16.0		
	23967	23955	1.002	493	0.994	12	11.9		
10	23951	23906	1.003	484	1.012	45	45.7	34.8	7.71
	23906	23877	1.005	492	0.996	29	29.0		
	23877	23847	1.006	498	0.984	30	29.7		
15	23801	23635	1.012	534	0.918	166	154	160	9.14
	23635	23464	1.019	454	0.992	171	173		
	23464	23312	1.026	500	0.980	152	153		
20	23731	23519	1.016	499	0.982	212	211	219	7.64
	23519	23290	1.025	535	0.916	229	215		
	23290	23070	1.035	487	1.006	220	229		
25	23972	23657	1.008	481	1.019	315	323	322	10.3
	23657	23355	1.021	489	1.002	302	309		
	23355	23032	1.035	490	1.000	323	334		
30	23552	23171	1.027	477	1.027	381	402	404	20.6
	23171	22759	1.045	490	1.000	412	431		
	22759	22407	1.063	482	1.017	352	380		
33	23680	23097	1.026	487	1.006	583	602	546	40.3
	23097	22597	1.050	488	1.004	500	527		
	22597	22124	1.073	489	1.002	473	509		
35	23726	23120	1.025	475	1.032	606	641	612	22.2
	23120	22540	1.051	490	1.000	580	610		
	22540	21996	1.078	490	1.000	544	586		
37	23808	23094	1.023	485	1.010	714	738	700	32.4
	23094	22406	1.055	506	0.968	688	703		
	22406	21804	1.086	486	1.008	602	659		
40	23888	22895	1.026	484	1.012	993	1031	962	53.0
	22895	22019	1.069	482	1.017	876	952		
	22019	21206	1.110	490	1.000	813	903		

Temp (deg C)	Dinitial	Dfinal	Cfsens	Tasm (sec)	Cftime	Praw	Poor	Avg Pops	Std Dev
45	21800	20727	1.129	488	1.004	1073	1216	1161	40.1
	20727	19787	1.185	476	1.029	940	1146		
	19787	18889	1.241	487	1.006	898	1121		
50	23834	22134	1.044	486	1.008	1700	1790	1557	194
	22134	20734	1.120	490	1.000	1400	1568		
	20734	19626	1.189	491	0.998	1108	1315		

Data for Temperature Tests for R-12

Temp (deg C)	Dinitial	Dfinal	Cfsens	Tasm (sec)	Cftime	Praw	Poor	Avg Pops	Std Dev
0	24000	23995	1.000	495	0.990	5	4.95	6.01	3.77
	23995	23993	1.000	485	1.010	2	2.02		
	23993	23982	1.001	487	1.006	11	11.1		
5	23991	23980	1.001	493	0.994	11	10.9	13.0	2.18
	23980	23964	1.001	491	0.998	16	16.0		
	23964	23952	1.002	493	0.994	12	11.9		
10	23951	23931	1.002	484	1.012	20	20.3	27.3	4.96
	23931	23900	1.004	492	0.996	31	31.0		
	23900	23869	1.005	498	0.984	31	30.6		
15	23883	23789	1.007	534	0.918	94	86.8	89.5	1.92
	23789	23698	1.011	494	0.992	91	91.2		
	23698	23607	1.015	500	0.980	91	90.5		
20	23859	23728	1.009	499	0.982	131	130	115	10.9
	23728	23607	1.014	535	0.916	121	112		
	23607	23506	1.019	487	1.006	101	104		
25	23985	23819	1.004	481	1.019	166	170	180	7.68
	23819	23641	1.011	489	1.002	178	180		
	23641	23456	1.019	490	1.000	185	189		
30	23769	23574	1.014	477	1.027	195	203	204	3.41
	23574	23378	1.022	490	1.000	196	200		
	23378	23179	1.031	482	1.017	199	209		
35	23879	23623	1.010	475	1.032	256	267	264	12.8
	23623	23351	1.022	490	1.000	272	278		
	23351	23112	1.033	490	1.000	239	247		
40	23969	23658	1.008	484	1.012	311	317	317	5.51
	23658	23346	1.021	482	1.017	312	324		
	23346	23046	1.035	490	1.000	300	310		

Appendix H
Data for Neutron Energy Tests

Data for Neutron Energy Tests for HFC-1 34A 5

En (MeV)	Charge (uC)	Sigma (mbams)	Fluence (n/cm2)	Resp (pops)	Temp (deg C)	Temp Corr	Corr Resp	Avg (pops)	Std Dev
0.09	223	250	55750	165	31.1	0.604	100	95	5.9
				161	31.0	0.608	98		
				141	30.9	0.612	86		
0.2	100	270	27000	582	30.8	0.616	358	349	6.8
				538	30.3	0.637	343		
				513	29.5	0.674	346		
0.55	20	510	10200	493	30.2	0.641	316	309	16
				458	28.8	0.710	325		
				416	29.2	0.689	287		
0.9	20	360	7200	420	30.3	0.637	267	245	18
				395	32.1	0.567	224		
				417	31.6	0.585	244		
1.3	20	290	5800	343	32.9	0.541	185	191	4.1
				299	30.0	0.650	194		
				304	30.3	0.637	194		
1.7	40	290	11600	605	30.5	0.628	380	374	5.1
				545	29.2	0.689	375		
				534	29.2	0.689	368		
2.1	20	290	5800	390	33.3	0.528	206	215	6.5
				395	32.6	0.550	217		
				381	31.7	0.581	221		
2.5	20	310	6200	271	26.5	0.861	233	197	37
				282	28.1	0.750	211		
				237	30.8	0.616	146		

En (MeV)	Resp/fluence (pops/(n/cm2))
0.09	0.0017
0.2	0.0129
0.55	0.0303
0.9	0.034
1.3	0.033
1.7	0.0323
2.1	0.0371
2.5	0.0318

Data for Neutron Energy Tests for R-12

En (Me)	Charge (uC)	Sigma (mbams)	Fluence (n/cm2)	Resp (pops)	Temp (deg C)	Temp Corr	Corr Resp	Avg (pops)	Std Dev
0.09	223	250	55750	8	31.1	0.604	4.83	7.10	1.8
				15	31.0	0.608	9.12		
				12	30.9	0.612	7.34		
0.2	100	270	27000	133	30.8	0.616	81.9	91.3	6.6
				150	30.3	0.637	95.5		
				143	29.5	0.674	96.4		
0.55	20	510	10200	346	30.2	0.641	222	230	9.4
				342	28.8	0.710	243		
				325	29.2	0.689	224		
0.9	20	360	7200	301	30.3	0.637	192	183	12
				293	32.1	0.567	166		
				325	31.6	0.585	190		
1.3	20	290	5800	239	32.9	0.541	129	153	17
				245	30.0	0.650	159		
				266	30.3	0.637	169		
1.7	40	290	11600	490	30.5	0.628	308	335	20
				510	29.2	0.689	351		
				504	29.2	0.689	347		
2.1	20	290	5800	310	33.3	0.528	164	168	4
				315	32.6	0.550	173		
				287	31.7	0.581	167		
2.5	20	310	6200	213	26.5	0.861	183	173	13
				242	28.1	0.750	181		
				251	30.8	0.616	155		

En (MeV)	Resp/fluence (pops/(n/cm2))
0.09	0.0001
0.2	0.0338
0.55	0.0225
0.9	0.0254
1.3	0.0263
1.7	0.0289
2.1	0.0290
2.5	0.0279

DISTRIBUTION LIST

DNA-TR-94-174

DEPARTMENT OF DEFENSE

ASSISTANT SECRETARY OF DEFENSE
INTERNATIONAL SECURITY POLICY
    ATTN: VERIFICATIONS POLICY

DEFENSE INTELLIGENCE AGENCY
    ATTN: DI-5
    ATTN: DIW-4
    ATTN: DT
    ATTN: PAM-1D

DEFENSE NUCLEAR AGENCY
 5 CY ATTN: OPAC LT COL B SIMELTON
 2 CY ATTN: SSTL

DEFENSE TECHNICAL INFORMATION CENTER
 2 CY ATTN: DTIC/OCP

FIELD COMMAND DEFENSE NUCLEAR AGENCY
    ATTN: FCPR

FIELD COMMAND DEFENSE NUCLEAR AGENCY
    ATTN: FCTO

ON-SITE INSPECTION AGENCY
 2 CY ATTN: OSIA/IAC MR WYCKOFF

DEPARTMENT OF THE NAVY

DEPARTMENT OF NAVAL ARCHITECTURE
 2 CY ATTN: B W BAKER
 2 CY ATTN: M E NELSON
 2 CY ATTN: M J HARPER

DEPARTMENT OF THE AIR FORCE

AIR UNIVERSITY LIBRARY
    ATTN: AUL-LSE

DEPARTMENT OF DEFENSE CONTRACTORS

JAYCOR
    ATTN: CYRUS P KNOWLES

KAMAN SCIENCES CORP
    ATTN: DASIAC

KAMAN SCIENCES CORPORATION
    ATTN: DASIAC